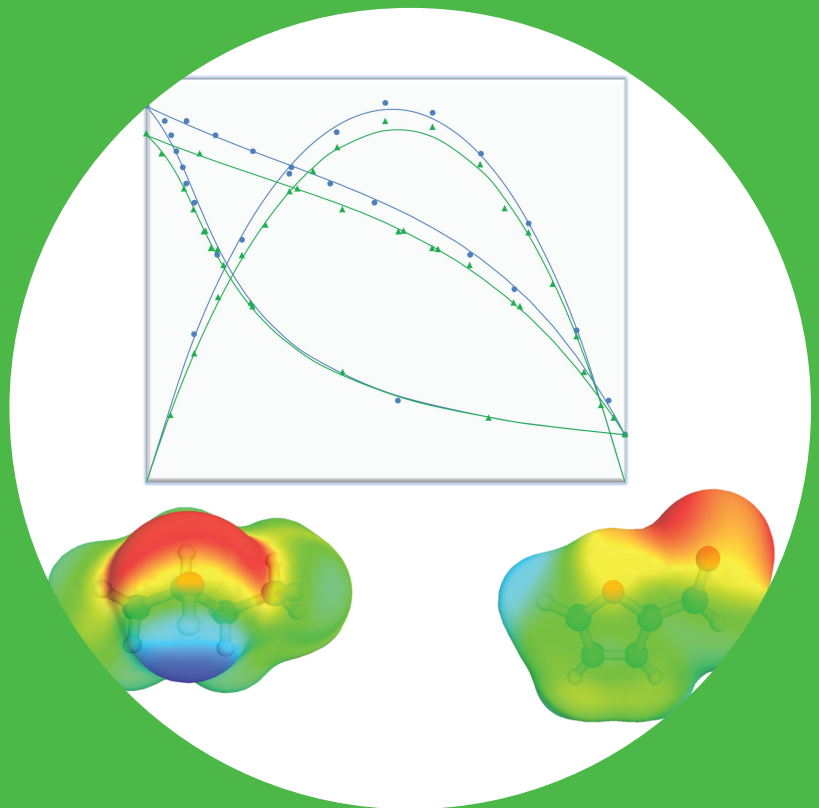


# Measurements and modeling of physical properties for oil and biomaterial refining

---

Anna Zaitseva



# Measurements and modeling of physical properties for oil and biomaterial refining

**Anna Zaitseva**

A doctoral dissertation completed for the degree of Doctor of Science (Technology) to be defended, with the permission of the Aalto University School of Chemical Technology, at a public examination held at the lecture hall KE2(Komppa Auditorium) of the school on 15 August 2014 at 12.

**Aalto University**  
**School of Chemical Technology**  
**Department of Biotechnology and Chemical Technology**  
**Research group of Chemical Engineering**

**Supervising professor**

Ville Alopaeus

**Thesis advisors**

D.Sc (Tech) Petri Uusi-Kyyny

D.Sc (Tech) Juha-Pekka Pokki

**Preliminary examiners**

Professor Jean Noël Jaubert, Université de Lorraine, France

Doctor Liudmila Mokrushina, Universität Erlangen-Nürnberg,  
Germany

**Opponent**

Professor Dr.-Ing. Wolfgang Arlt, Universität Erlangen-Nürnberg,  
Germany

Aalto University publication series

**DOCTORAL DISSERTATIONS** 94/2014

© Anna Zaitseva

ISBN 978-952-60-5750-7

ISBN 978-952-60-5751-4 (pdf)

ISSN-L 1799-4934

ISSN 1799-4934 (printed)

ISSN 1799-4942 (pdf)

<http://urn.fi/URN:ISBN:978-952-60-5751-4>

Unigrafia Oy

Helsinki 2014

Finland

Publication orders (printed book):

<https://aaltodoc.aalto.fi/>



**Author**

Anna Zaitseva

**Name of the doctoral dissertation**

Measurements and modeling of physical properties for oil and biomaterial refining

**Publisher** School of Chemical Technology

**Unit** Department of Biotechnology and Chemical Technology

**Series** Aalto University publication series DOCTORAL DISSERTATIONS 94/2014

**Field of research** Chemical Engineering

**Manuscript submitted** 8 April 2014

**Date of the defence** 15 August 2014

**Permission to publish granted (date)** 17 June 2014

**Language** English

**Monograph**

**Article dissertation (summary + original articles)**

**Abstract**

The aim of this thesis was to investigate a set of binary systems for developing necessary thermodynamic models for oil and biofuel industries. Extensive experimental work was performed for supplying the necessary vapor – liquid equilibria (VLE) and excess enthalpy data for the selected systems.

Binary systems with C4 hydrocarbons + alkenes, alcohols and ketones were measured due to their importance in production of fuel additives. Static total pressure apparatus was utilized for these isothermal measurements. Important for fuel purification, systems with sulfur containing compounds were measured using recirculation still apparatus at isothermal conditions. Several experimental techniques for VLE measurements were applied for investigation of furfural containing binary systems and for the 2-methoxy-2-methylpropane (MIBK) + alcohol systems. Furfural can serve as one of the precursor in production of biofuel. Calorimetric measurements were also made for these systems using flow mixing calorimeter. Consistency of all experimental data was analyzed with four different consistency tests.

The obtained experimental data were used for optimization of Wilson, NRTL an UNIQUAC model parameters and for validation of predictive group contribution model UNIFAC(Dortmund) and predictive COSMO-RS model.

A method for improving group contribution methods is suggested. The distance weighting technique takes into account similarity of the compounds for optimization of the group contribution parameters. The suggested method is applicable to linearized group contribution methods. Normal boiling points of the pure compounds were predicted applying new technique to Joback – Reid and Marrero – Gani group contribution methods. Average improvement of the normal boiling point predictions was 6 K for the Joback – Reid method and 4 K for the Marrero – Gani method.

**Keywords** vapor-liquid equilibrium, excess enthalpy, furfural, COSMO-RS, UNIFAC, headspace gas chromatograph, recirculation still apparatus, static total pressure apparatus

**ISBN (printed)** 978-952-60-5750-7

**ISBN (pdf)** 978-952-60-5751-4

**ISSN-L** 1799-4934

**ISSN (printed)** 1799-4934

**ISSN (pdf)** 1799-4942

**Location of publisher** Helsinki

**Location of printing** Helsinki

**Year** 2014

**Pages** 228

**urn** <http://urn.fi/URN:ISBN:978-952-60-5751-4>



## Preface

This thesis is the result of the many years of research that I have been carrying out at the Laboratory of Chemical Engineering and Plant Design of Helsinki University of Technology, and later Aalto University. It wouldn't have been possible without the help and support of many individuals and organizations.

I would like to thank TEKES (National Technology Agency of Finland) and the industrial partners for funding the BIOSCEN project, and the Academy of Finland for their financial support of the project "Phase Stability Calculation and Equilibrium Measurements for a Biorefinery". I am grateful to the Finnish IT Center of Science (CSC) and Dr. Nino Runeberg for the computing resources and assistance provided to perform the quantum calculations.

I was very lucky to work under the supervision of Professor Juhani Aittamaa. I would like to thank him for the suggestion to start my postgraduate study at his laboratory, for all the help he gave me through the years of his supervision, and for the unforgettable atmosphere that he created in the laboratory.

I would also like to acknowledge the valuable help of my current supervisor Professor Ville Alopaeus, whose splendid ideas and wise guidance gave me the opportunity to complete this work.

I wish to thank all eleven of my co-authors: without you this thesis would have been impossible! I am grateful to you for having the courage to explore a new predictive method, and your patience in discussing this topic with me. My thanks also go to Dr. Helena Laavi, who gave me an example of well-organized work, provided good comments on my manuscripts and supported me in studying the Finnish language. I appreciate the extensive contribution of Dr. Erlin Sapei to this thesis, thank you Erlin for our cooperation in writing the articles dedicated to sulfur-containing compounds. My warm thanks to Minna Pakkanen and Piia Haimi for their help in everyday life in the laboratory.

I am greatly indebted to Dr. Petri Uusi-Kyyny, whose optimism and knowledge gave me the strength to overcome difficulties in the experimental work. My special thanks go to Dr. Juha-Pekka Pokki for wisely guiding my research during recent years and his readiness to discuss any problems I encountered. I respect both of you for your enthusiasm, curiosity and confidence, which made this work possible.

I thank all my dearest former and present colleagues from the laboratory for the entertaining conversations in the coffee room, the inspiring work atmosphere and many small but indispensable occasions where you helped me. I am also extremely grateful to my friends Piia Haimi, Claudia Dell'Era, and Alexey Zakharov for their practical help, moral support, and fun conversations.

I appreciate very much the help of Sirpa Aaltonen and Lasse Westerlund on the administrative issues.

Finally, my warmest thanks to my husband Igor and to my sunny sons Nikita and Jyri for being with me and for their love.

## List of publications

- I. Zaitseva, A. and Alopaeus, V. Improving group contribution methods by distance weighting | Amélioration de la méthode de contribution du groupe en pondérant la distance du groupe. **Oil and Gas Science and Technology** (2013), vol. 68, no. 2, pp. 235-247.
- II. Zaitseva, A.; Laavi H.; Pokki J.-P.; Uusi-Kyyny P. and Alopaeus V. Isothermal Vapor-Liquid Equilibrium and Excess Molar Enthalpies of the binary mixtures furfural + methyl isobutyl ketone, + 2-butanol and + 2-methyl-2-butanol, accepted to **Fluid Phase Equilibria** 18.03.2014 with minor revisions.
- III. Laavi, H.; Zaitseva, A.; Pokki, J.-P.; Uusi-Kyyny, P.; Kim, Y.; Alopaeus, V. Vapor-liquid equilibrium, excess molar enthalpies, and excess molar volumes of binary mixtures containing methyl isobutyl ketone (MIBK) and 2-butanol, tert-pentanol, or 2-ethyl-1-hexanol. **Journal of Chemical and Engineering Data** (2012), vol. 57, n. 11, pp. 3092-3101.
- IV. Zaytseva, A.; Uusi-Kyyny, P.; Pokki, J.-P.; Pakkanen, M.; Aittamaa, J. Vapor-Liquid Equilibrium for the trans-2-Butene + Methanol, + Ethanol, + 2-Propanol, + 2-Butanol, and + 2-Methyl-2-propanol Systems at 332 K. **Journal of Chemical and Engineering Data** (2004), 49(5), 1168-1174.
- V. Dell'Era, C.; Zaytseva, A.; Uusi-Kyyny, P.; Pokki, J.-P.; Pakkanen, M.; Aittamaa, J. Vapour-liquid equilibrium for the systems butane + methanol, +2-propanol, +1-butanol, +2-butanol, +2-methyl-2-propanol at 364.5 K. **Fluid Phase Equilibria** (2007), 254(1-2), 49-59.
- VI. Pasanen, M.; Zaytseva, A.; Uusi-Kyyny, P.; Pokki, J. -P.; Pakkanen, M.; Aittamaa, J. Vapor Liquid Equilibrium for Six Binary Systems of C4-Hydrocarbons + 2-Propanone. **Journal of Chemical & Engineering Data** (2006), 51(2), 554-561.
- VII. Ouni, T.; Zaytseva, A.; Uusi-Kyyny, P.; Pokki, J.-P.; Aittamaa, J. Vapour-liquid equilibrium for the 2-methylpropane + methanol, +ethanol, +2-propanol, +2-butanol and +2-methyl-2-propanol systems at 313.15K. **Fluid Phase Equilibria** (2005), 232(1-2), 90-99.
- VIII. Sapei, E.; Zaytseva, A.; Uusi-Kyyny, P.; Younghun, K.; Keskinen, K. I.; Aittamaa, J. Vapor-Liquid Equilibrium for Binary System of 1-Propanethiol, Thiophene, and Diethyl Sulfide with Toluene at 90.03 kPa. **Journal of Chemical & Engineering Data** (2006), 51(4), 1372-1376.
- IX. Sapei, E.; Zaytseva, A.; Uusi-Kyyny, P.; Keskinen, K. I.; Aittamaa, J. Vapor-Liquid Equilibrium for Binary System of Diethyl Sulfide + n-Hexane at (338.15 and 323.15) K and Diethyl Sulfide + 1-Hexene at (333.15 and 323.15) K. **Journal of Chemical & Engineering Data** (2007), 52(2), 571-576.
- X. Sapei, E.; Zaytseva, A.; Uusi-Kyyny, P.; Keskinen, K. I.; Aittamaa, J. Vapor-Liquid Equilibrium for Binary System of Diethyl Sulfide + n-Heptane and Diethyl Sulfide + 2,2,4-Trimethylpentane at (363.15 and 353.15) K. **Journal of Chemical & Engineering Data** (2007), 52(1), 192-198.

- XI. Sapei, E.; Zaytseva, A.; Uusi-Kyyny, P.; Keskinen, K. I.; Aittamaa, J. Vapor-liquid equilibrium for binary system of diethyl sulfide + cyclohexane at 353.15 and 343.15K and diethyl sulfide + 2-ethoxy-2-methylpropane at 343.15 and 333.15K. **Fluid Phase Equilibria** (2007), 252(1-2), 130-136.
- XII. Sapei, E.; Zaytseva, A.; Uusi-Kyyny, P.; Keskinen, K. I.; Aittamaa, J. Vapor-Liquid Equilibrium for Binary System of Thiophene + n-Hexane at (338.15 and 323.15) K and Thiophene + 1-Hexene at (333.15 and 323.15) K. **Journal of Chemical & Engineering Data** (2006), 51(6), 2203-2208.
- XIII. Sapei, E.; Zaytseva, A.; Uusi-Kyyny, P.; Keskinen, K. I.; Aittamaa, J. Vapor-liquid equilibrium for binary system of thiophene+2,2,4-trimethylpentane at 343.15 and 353.15K and thiophene+2-ethoxy-2-methylpropane at 333.15 and 343.15K. **Fluid Phase Equilibria** (2007), 261(1-2), 115-121.



## Statement of the author's contribution to the appended publications

I. The author developed the model together with Professor Alopaeus, tested the model on an available database and wrote the paper.

II. The author designed the procedure for furfural treatment within the measurements, distilled chemicals for the measurements, made static total pressure measurements, recirculation still measurements, headspace GC measurements, participated in excess enthalpy measurements, analyzed the reagent and made an analysis of the furfural purity, modeled the data and wrote the manuscript.

III. The author distilled chemicals for the measurements, set up and performed headspace gas chromatography measurement, and participated in writing the manuscript.

IV. The author analyzed the results, modeled the systems, and wrote the paper together with Mr Uusi-Kyyny, D.Sc.

V. – VII The author performed the COSMO quantum calculations and conformation analysis for twelve molecules under consideration. The author did predictions of VLE for the sixteen binary systems using the obtained COSMO-RS sigma profiles and compared the results with the static total pressure apparatus experimental data. The author participated in writing the manuscript.

VIII – XIII. The author did conformational search and COSMO quantum calculations for the considered in the articles ten molecules, performed COSMO-RS modeling for the thirteen binary systems and compared the results with the circulation still apparatus VLE data and the literature excess enthalpy data. The author participated in writing the manuscript.

## Notations

<i>A</i>	area
<i>a</i>	temperature dependent parameters of NRTL, Wilson and UNIQUAC models
<i>D</i>	area consistency test criterion
<i>E</i>	energy
<i>F</i>	consistency test parameters
<i>f</i>	fugacity
<i>G</i>	Gibbs free energy
<i>g</i>	molar Gibbs free energy
<i>H</i>	enthalpy
<i>h</i>	molar enthalpy
<i>I</i>	infinite dilution consistency test criterion
<i>N</i>	number of molecules or total number of experimental points
<i>n</i>	number of moles
<i>P</i>	pressure
<i>P<sub>i</sub></i>	partial pressure
<i>Q</i>	quality factor
<i>q</i>	surface area parameter
<i>R</i>	gas constant
<i>r</i>	volume parameter
<i>S</i>	entropy
<i>s</i>	molar entropy
<i>T</i>	temperature
<i>u</i>	energy parameters of NRTL, Wilson and UNIQUAC models
<i>V</i>	volume
<i>v</i>	molar volume
<i>X</i>	vector of molar compositions
<i>x</i>	liquid mole fraction
<i>y</i>	vapor mole fraction
<i>Z</i>	partition function
<i>z</i>	total mole fraction
<i>z</i>	average coordination number in UNIQUAC model

## Abbreviations

AARE	absolute average relative error
AZE	azeotrope
BP	Becke Perdew functional
DFT	density functional theory
EOS	equation of state
ETBE	2-ethoxy-2-methylpropane, CAS# 637-92-3
FID	flame ionization detector
GC	gas chromatograph
HB	hydrogen bond
HS	head space gas chromatography
LEG	Legendre polynomial activity coefficient model
MIBK	Methyl Isobutyl Ketone, CAS# 108-10-1
NRTL	nonrandom two liquid model
PM3	Semiempirical QM model “Parameterized Model 3”
QM	quantum method
RI	resolution of identity
SRK	Soave-Redlich-Kwong
TZVP	triple-zeta valence potential basis set
tert-pentanol	2-methyl-2-butanol, CAS# 75-85-4
UNIF	UNIFAC activity coefficient model
UNIFD	UNIFAC (Dortmund) activity coefficient model
UNIQUAC	Universal quasichemical activity coefficient model
VLE	vapor – liquid equilibrium
Wil	Wilson activity coefficient model

### Greek letters

$\alpha$	non-randomness parameter of NRTL model
$\varepsilon$	interaction energy
$\phi$	volume fraction
$\delta$	differential consistency test criterion
$\gamma$	activity coefficient
$\varphi$	fugacity coefficients
$\Lambda$	Wilson model parameters
$\mu$	chemical potential
$\mu, \nu$	segment index
$\theta$	surface area fraction
$\rho$	density
$\sigma$	surface charge
$\tau, \tau'$	parameters of NRTL or UNIQUAC model

### Subscripts and Superscripts

<i>acc</i>	acceptor
<i>C</i>	combinatorial
<i>calc</i>	calculated
<i>cell</i>	static total pressure apparatus cell
<i>E</i>	excess property
<i>eff</i>	effective
<i>exp</i>	experimental
<i>IG</i>	ideal gas
<i>IM</i>	ideal mixture
<i>i, j, m</i>	component
<i>k</i>	measurement index
<i>L</i>	liquid phase
<i>l</i>	consistency test index
<i>lit</i>	literature
<i>pump</i>	syringe pump
<i>R</i>	residual
<i>sat</i>	saturated
<i>V</i>	vapor phase
<i>vdW</i>	van der Waals
<i>0</i>	standard state
$\bar{\phantom{x}}$	partial property
$\infty$	infinite dilution

## Table of Contents

<b>1. Introduction</b> .....	<b>1</b>
<b>2. Thermodynamic background</b> .....	<b>3</b>
2.1. Thermodynamic principles of phase equilibrium .....	3
2.2. Activity coefficient models .....	5
2.3. Consistency of the experimental data .....	6
2.4. Quality factor of the experimental data .....	8
2.5. Theoretical background of the UNIFAC and COSMO-RS models .....	9
2.5.1. UNIFAC (UNIQUAC Functional-group Activity Coefficients) model .....	10
2.5.2. COSMO-RS (COnductor-like Screening Model for Real Solvents) .....	10
<b>3 Results and discussion</b> .....	<b>14</b>
<b>3.1 Experimental measurements</b> .....	<b>16</b>
3.1.1 Static total pressure apparatus .....	16
3.1.2 Reduction of the static total pressure apparatus data .....	18
3.1.3 Uncertainty of the static total pressure apparatus data .....	18
3.1.4 Results of the static total pressure apparatus data .....	20
3.1.5 Recirculation still apparatus .....	22
3.1.6 Uncertainty of the recirculation still data .....	23
3.1.7 Results of the recirculation still data .....	23
3.1.8 Headspace gas chromatography (HS) .....	25
3.1.9 Reduction of headspace gas chromatographic data .....	27
3.1.10 Uncertainty of headspace gas chromatographic data .....	28
3.1.11 Results of headspace gas chromatographic data .....	28
3.1.12 Calorimetry .....	30
3.1.13 Uncertainty of calorimetric measurements .....	30
3.1.14 Results of the calorimetric measurements .....	31

3.1.15	Gas chromatography .....	32
<b>3.2</b>	<b>Comparison of measurement techniques used.....</b>	<b>32</b>
<b>3.3</b>	<b>Optimization of the Activity coefficient model parameters.....</b>	<b>34</b>
<b>3.4</b>	<b>Prediction of VLE with UNIFD and COSMO-RS predictive models.....</b>	<b>34</b>
3.4.1	Details of the COSMO-RS calculations.....	36
3.4.2	Alcohols .....	42
3.4.3	Ketones.....	46
3.4.4	Diethyl sulfide .....	50
3.4.5	Thiophene.....	53
3.4.6	Furfural.....	55
<b>3.5</b>	<b>Prediction of excess enthalpies with the UNIFAC-Dortmund and COSMO-RS models.....</b>	<b>59</b>
<b>3.6</b>	<b>Improvement of group contribution methods by distance weighting .....</b>	<b>64</b>
<b>4</b>	<b>Conclusions.....</b>	<b>66</b>
	<b>References .....</b>	<b>68</b>

## 1. Introduction

Complex mathematical modeling of chemical processes is being applied more and more for research and development of new and existing production technologies. Nowadays, a multi-stage process can be modeled with good accuracy by utilizing thermodynamics and heat and mass balances for each process unit. Successful simulation allows the evaluation of different process options for optimization of process costs and for delivering a product of better quality. Various phenomena have to be taken into account for reliable modeling of each process unit. In particular, a complicated description is required for processes where mass and heat transfers occur simultaneously with chemical reactions and phase equilibria. Phase equilibria and the component thermodynamic properties determine the theoretical feasibility of the process. Therefore, reliable experimental or predicted thermodynamic data are of major importance.

Thermodynamics establish the fundamental relationships between the physical variables of a chemical system. However, the application of these principles requires knowledge of thermodynamic potentials or the internal energies of the chemical system (such as Helmholtz or Gibbs energies) that are determined by the microscopic behavior of the system. Over the years, chemists and engineers have developed simplified descriptions of these energy variables using thermodynamic models. The thermodynamic models utilize data that were measured previously for extrapolation and interpolation of the chemical system behavior to other conditions. Some of the thermodynamic models require optimization of the parameters for each chemical system based on available experimental data (such as NRTL or UNIQUAC models). Other models assume that the system behavior does not depend on the compounds of the mixture, but on the smaller molecule units, i.e. groups. In this case, the system behavior is determined by interactions of functional groups or surface segments and their sizes (like in UNIFAC or COSMO-RS). Thus, the extrapolation of the thermodynamic behavior can be made not only for other operating conditions, but also for other chemicals composed of known types of groups. Models that utilize this approach are called predictive models.

The main goals of this work were the development of thermodynamic models based on new experimental data and evaluation of the existing predictive models with the obtained data. Within the scope of the work, a novel technique for improving group contribution predictive methods was studied. In publications I, it was shown that more extensive use of available experimental data in

group contribution predictive methods (like Joback – Reid or Marrero – Gani) increases the accuracy of normal boiling point prediction.

Extensive experimental work was performed to provide experimental vapor-liquid equilibrium data for industrially relevant binary systems, for which the experimental data were unavailable or scarce. The accuracy of the measured data was evaluated and the thermodynamic model parameters were optimized based on the measured data. UNIFAC – Dortmund and COSMO-RS predictive models were evaluated for their ability to forecast the thermodynamic behavior of the same binary system.

The systems of interest were the components of gasoline and biofuel production. There are several major challenges related to the worldwide use of gasoline. One of the problems is the reduction of exhaust emissions from combustion engines into the atmosphere. Aside from the possible greenhouse effects of exhaust gases, some of the emitted compounds (carbon monoxide, sulfur-containing compounds) can be toxic to humans and the environment. Another challenge is the development of a renewable fuel that inherits the best properties of the modern fossil fuel, i.e. liquid state, high energy density, and low cost. In this work, a set of thermodynamic data was measured and modeled. The data obtained are useful and necessary information for production of a fuel additive [IV - VII], separation of sulfur-containing compounds from crude oil [VIII-XIII], and production of alternative fuels [II, III].

## 2. Thermodynamic background

### 2.1. Thermodynamic principles of phase equilibrium

The main principle of phase equilibrium is that the Gibbs energy of the system is at its minimum. The Gibbs energy is a function of temperature, pressure, and composition

$$dG = -SdT + VdP + \sum_{i=1}^c \bar{G}_i dN_i, \quad (2.1.1)$$

As a reference point for the estimation of the Gibbs energy, the Gibbs energy of pure ideal gas ( $G_i^{IG}$ ) can be used. The minimum of the Gibbs energy can be replaced with the equality of the fugacities of the phases, which are defined as

$$f_i = P_i \cdot \exp\left\{\frac{\bar{G}_i(T,P,X) - G_i^{IG}(T,P)}{RT}\right\}. \quad (2.1.2)$$

Thus the equilibrium condition becomes  $f_i^V = f_i^L$

The fugacity is a measure of the system non-ideality. The non-ideality can be more clearly expressed through the fugacity coefficient [1]

$$\varphi_i = \frac{f_i}{P_i} = \exp\left\{\frac{\bar{G}_i(T,P,X) - G_i^{IG}(T,P)}{RT}\right\} \quad (2.1.3)$$

Taking into account that  $P_i = x_i P$ , the equilibrium condition becomes  $y_i \varphi_i^V = x_i \varphi_i^L$ .

This approach to equilibrium calculations is called the  $\varphi - \varphi$  approach. At constant temperature and composition, in accordance with eq. (2.1.1) and (2.1.3), the fugacity coefficient can be found by integrating the partial molar volume of an ideal gas and the partial molar volume of real system from zero pressure to the pressure of the system. For example, an equation of state (EOS) describes the dependency of the partial molar volume of the system on pressure and its integration with pressure gives us the desired fugacity coefficients.

For liquid solutions, fugacity of the pure liquid  $i$  at system temperature and pressure ( $f_i^{L,0}$ ) is commonly used as a reference state. Thus, another characteristic of the liquid non-ideality can be applied, i.e. the activity coefficient. The fugacity of the liquid can then be expressed as

$$f_i^L = x_i \gamma_i f_i^{L,0}, \quad (2.1.4)$$



The required fugacity  $f_i^{L,0}$  can be found by correcting the saturated liquid fugacity with the Poynting correction. The Poynting correction takes into account the change in the liquid fugacity from the saturated liquid pressure to the system vapor pressure.

$$f_i^{L,0} = f_i^{L,sat} \exp\left(\int_{P_{sat}}^P \frac{v_i^L}{RT} dP\right)$$

Finally, the equilibrium condition for this ( $\gamma - \phi$ ) approach becomes

$$y_i \phi_i P = x_i \gamma_i f_i^{L,0} = x_i \gamma_i P_i^{sat} \phi_i^{sat} \exp\left(\int_{P_{sat}}^P \frac{v_i^L}{RT} dP\right) \quad (2.1.5)$$

In the oil refinery, EOS are commonly used for description of VLE ( $\phi - \phi$  approach) and activity coefficient models can be utilized in new generation of EOS to generate effective mixing rules [2-4]. However, in our publications, traditional  $\gamma - \phi$  approach is used due to its simplicity and low pressures under study.

In most cases, the Soave-Redlich-Kwong EOS [5] was applied with zero binary interaction parameters to describe the vapor phase. The pure liquid molar volumes were obtained from the Rackett correlation [6] and the Wilson, UNIQUAC and NRTL models were applied to calculate activity coefficients of components in the liquid phase. The interaction parameters of the activity coefficient models have been fitted to experimental data and thus are valid for the temperatures at which the equilibrium measurements were made. The temperature range of the parameters can be extended by taking into account the dependency of the activity coefficients on temperature based on the calorimetric measurements.

For deducing the equation used in calorimetry, the activity coefficient (2.1.4) and fugacity as a function of Gibbs energy (2.1.2) are combined. Thus, it can be shown [1] that the partial molar excess Gibbs energy is a measure of the activity coefficients  $\gamma_i = \exp\left(\frac{G_i^E}{RT}\right)$ . (2.1.6)

By definition, the Gibbs free energy is related to enthalpy,  $G = H - TS$ , and the derivative of the Gibbs energy at constant pressure is entropy  $S = -\left(\frac{\partial G}{\partial T}\right)_P$ . Using the last two equations and an equation for the partial molar excess property,  $\bar{M}_i^E = \bar{M}_i - \bar{M}_i^{IM}$ , we obtain

$$\frac{\partial}{\partial T} \left(\frac{G_i^E}{T}\right)_{P,x} = -\frac{H_i^E}{T^2} \quad (2.1.7)$$

Substituting equation (2.1.6) into (2.1.7) gives

$$\left(\frac{\partial \ln \gamma_i}{\partial T}\right)_{P,X} = -\frac{\bar{H}_i^E}{RT^2} \quad (2.1.8)$$

When the partial molar excess enthalpy is assumed to be temperature independent, the activity coefficients at one temperature can be used for predicting the activity coefficient at another temperature, with the following equation:

$$\gamma_i(T_2, P, X) = \gamma_i(T_1, P, X) \cdot \exp\left[\frac{\bar{H}_i^E(T,P,X)}{R}\left(\frac{1}{T_2} - \frac{1}{T_1}\right)\right] \quad (2.1.8)$$

## 2.2. Activity coefficient models

The following excess Gibbs energy models were used to describe the activity coefficients (see equations 2.1.5, 2.1.6 and 2.1.8): Wilson, UNIQUAC, and NRTL. The excess Gibbs energy equations of the models for two component systems are

$$\frac{g^E}{RT} = -x_1 \cdot \ln(x_1 + x_2 \Lambda_{12}) - x_2 \cdot \ln(x_2 + x_1 \Lambda_{21}) \quad (2.2.1) \quad \text{Wilson}$$

where  $g^E$  is the molar excess Gibbs energy and  $\Lambda_{12}$  and  $\Lambda_{21}$  are Wilson parameters that can be modeled with an additional temperature dependence as

$$\Lambda_{ij} = \frac{v_i^L}{v_j^L} \exp\left(-\frac{u_{ij}-u_{jj}}{RT}\right), \text{ where } (u_{ij} - u_{jj})/R = a_{o,ij} + a_{1,ij} \cdot T + a_{2,ij} \cdot T^2$$

Different weighting of the mole fraction in the molar excess Gibbs free energy will give us another widely used activity coefficient model – NRTL:

$$\frac{g^E}{RT} = x_1 x_2 \left( \frac{\tau_{21} G_{21}}{x_1 + x_2 G_{21}} + \frac{\tau_{12} G_{12}}{x_2 + x_1 G_{12}} \right) \quad (2.2.3) \quad \text{NRTL}$$

where  $G_{ij} = \exp(-\alpha \tau_{ij})$ ,  $\tau_{ij} = (u_{ij} - u_{jj})/RT$

Additionally, the  $u_{ij}$  parameters can be treated as temperature dependent and  $\tau_{ij}$  becomes:

$$\tau_{ij} = (a_{o,ij} + a_{1,ij} \cdot T + a_{2,ij} \cdot T^2)/T \quad (2.2.4)$$

The  $\alpha$  parameter is usually considered to be constant and describes the degree of local order of molecules.

These local composition models (Wilson, NRTL) assume that the entropy and enthalpy contributions to the molar excess enthalpy depend on the mole fractions of the compounds. It can lead to some difficulties in describing molecules of different size, where the excess entropy seems to correlate better with the volume fraction. Additionally, the intermolecular interactions seem to be related to the type and availability of the molecule surface, but not to the molecule fractions. The UNIQUAC model integrated these ideas in the following equation for the molar excess Gibbs energy:

$$\frac{g^E}{RT} = \sum_i x_i \ln \frac{\phi_i}{x_i} + \frac{z}{2} \sum_i x_i q_i \ln \frac{\theta_i}{\phi_i} - \sum_i q_i x_i \ln \left( \sum_j \theta_j \tau'_{ji} \right) \quad (2.2.5) \text{ UNIQUAC}$$

where  $z$  is the average coordination number (usually taken to be 10);  $\theta_i$  is the surface area fraction of species  $i$ ,  $\theta_i = x_i q_i / \sum_j x_j q_j$ ;  $q_i$  is the surface area parameter for species  $i$ ;  $\phi_i$  is the volume fraction of species  $i$ ,  $\phi_i = x_i r_i / \sum_j x_j r_j$  and  $r_i$  is the volume parameter for species  $i$ ;  $\tau'_{ji} = \exp\left(-\frac{u_{ij}-u_{jj}}{RT}\right)$ . The interaction parameter  $\tau'_{ij}$  can be expressed as in the NRTL model (2.2.4) with additional temperature dependency.

### 2.3. Consistency of the experimental data

The basic thermodynamics provide a way to estimate the accuracy of measurements. The most often applied consistency test is the area test.

When equation 2.1.1. is applied to excess Gibbs energy, we obtain

$$dG^E = \left(\frac{\partial G^E}{\partial T}\right)_{P, N_i} dT + \left(\frac{\partial G^E}{\partial P}\right)_{T, N_i} dP + \sum \left(\frac{\partial G^E}{\partial N_i}\right)_{T, P} dN_i$$

Taking into account eq. (2.1.6), (2.1.7) and that  $\left(\frac{\partial G^E}{\partial P}\right)_{T, N_i} = v^E$ , one can get for a binary system

$$\frac{dg^E}{RT} = -\frac{h^E}{RT^2} dT + \frac{v^E}{RT} dP + \ln \frac{\gamma_1}{\gamma_2} dx_1 \quad (2.3.1)$$

This equation can be integrated over the whole range of composition ( $x_1$ ), from 0 to 1. The result of the integration is zero, since the left-hand side of eq. (2.3.1) gives zero due to the zero integration limits  $g^E(x_1=1)$  and  $g^E(x_1=0)$ . This condition is valid for all consistent thermodynamic models and for consistent measured data.

At isothermal conditions, integration of the right-hand side of equation (2.3.1) over composition  $x_1$  gives

$$\int_0^1 \ln \frac{\gamma_1}{\gamma_2} dx_1 + \int_0^1 \left( \frac{v^E}{RT} \right) \left( \frac{\partial P}{\partial x_1} \right)_T dx_1 = 0 \quad (2.3.2)$$

The second integral in equation (2.3.2) is usually small and can be neglected [7], thus the deviation of the first integral of (2.3.2) from zero is a measure of the thermodynamic consistency of the isothermal data. In a similar way, the consistency of the isobaric data can be checked using equation (2.3.3), but the second integral in equation (2.3.3) is not negligible in this case.

$$\int_0^1 \ln \frac{\gamma_1}{\gamma_2} dx_1 - \int_0^1 \left( \frac{h^E}{RT^2} \right) \left( \frac{\partial T}{\partial x_1} \right)_P dx_1 = 0 \quad (2.3.3)$$

When the  $h^E$  is available or correlated empirically, the second integral of eq. (2.3.3) can be estimated. Equations (2.3.2) and (2.3.3) are the basis for the area test. It has been generally accepted that for good quality data, the deviation of  $\int_0^1 \left| \ln \frac{\gamma_1}{\gamma_2} \right| dx_1$  from 0 should be less than 5% for eq. (2.3.2) and less than 10% - for eq. (2.3.3).

Another consistency test (the Van Ness test) uses the deviation between the experimental and model values of the measured thermodynamic variables as the test criteria. Obviously, common thermodynamic models do not contradict the thermodynamic laws. Thus, data with no deviation from the model is thermodynamically consistent. However, such test results are not always correct, because deviation of data from the model could be due to the inapplicability of the model to the modeled system. At the same time, both the model and the data could be thermodynamically consistent. 1% is conventionally accepted as a limit for the average deviation in pressure or vapor mole fractions between measured and modeled values.

The differential or point test is the test of the differential properties of molar excess Gibbs energy data. In accordance with equation (2.1.6), the molar excess Gibbs energy in a binary system equals

$$\frac{g^E}{RT} = x_1 \ln \gamma_1 + x_2 \ln \gamma_2 \quad (2.3.4)$$

and its differential at constant temperature is equal to

$$d(g^E/RT) = \ln \frac{\gamma_1}{\gamma_2} dx_1 + \left( \frac{v^E}{RT} \right) \left( \frac{\partial P}{\partial x_1} \right)_T dx_1 \quad (2.3.5)$$

The last term of equation (2.3.5) can be neglected [7] and equation (2.3.5) can be calculated at each experimental concentration:

$$\left. \frac{\partial(g^E/RT)}{\partial x_1} \right|_{x_k} - \ln \frac{\gamma_1}{\gamma_2} \Big|_{x_k} = 0 = \delta_k \quad (2.3.6)$$

The logarithmic part of eq. (2.3.6) is a derivative of the  $g^E$  function calculated from the experimental data. On the other hand, the  $g^E$  function can be calculated with eq. (2.3.4) and described by a polynomial function dependent on  $x_i$ . To estimate the quality of the  $g^E$  function description, the polynomial fitted to the  $g^E$  function is differentiated analytically and the  $\delta_k$  is calculated for each experimental composition. Finally, the average percentage value of  $\delta_k$  is a test parameter that reveals the quality of the  $g^E$  function measurements. This test is not applicable to isobaric data for the same reasons that were mentioned for the area test.

The infinite dilution test shows the accuracy of molar excess Gibbs energy measurements in diluted regions ( $x_1 \rightarrow 0$  and  $x_2 \rightarrow 0$ ). In the infinite dilution region ( $x_1 \rightarrow 0$ ), in accordance with eq. (2.3.4), the following equation is valid:

$$\lim_{x_1 \rightarrow 0} \left( \frac{g^E}{x_1 x_2 RT} \right) = \lim_{x_1 \rightarrow 0} \left( \ln \frac{\gamma_1}{\gamma_2} \right) = \lim_{x_1 \rightarrow 0} (\ln \gamma_1) = \ln \gamma_1^\infty$$

Based on this equality the following criteria were suggested by Kojima et al. [7]:

$$I_{i, i \neq j} = 100 \left| \frac{\frac{g^E}{x_1 x_2 RT} - \ln \frac{\gamma_i}{\gamma_j}}{\ln \frac{\gamma_i}{\gamma_j}} \right|_{x_i \rightarrow 0} \quad I_i \leq 30 \quad (2.3.7)$$

where both  $g^E/(x_1 x_2 RT)$  and  $\ln(\gamma_i/\gamma_j)$  are approximated by polynomial functions.

## 2.4. Quality factor of the experimental data

All four of the described criteria can be combined in the data quality factor  $Q$  as it is described in [8] and publication II. In the  $Q$  factor, the precision of the pure component vapor pressure measurements is also taken into account as it has a considerable effect on the calculations of activity coefficients, eq. (2.1.5).

The quality factor in accordance with Kang et al. [8] can be calculated from the parameters of each consistency test mentioned above ( $F_i$ , where  $i=Area$  or  $Van$  Ness or  $point$  or  $\infty$ ) in accordance with the following equation:

$$Q = F_{pure} \cdot (F_{Area} + F_{VanNess} + F_{point} + F_{\infty}) \quad (2.3.9)$$

Each parameter is calculated with the consistency test criteria:

$$F_{Area} = 1.25/D \quad D = 100 \left| \frac{A_1 - A_2}{A_1 + A_2} \right| \quad \begin{aligned} A_1 &= \left| \int_0^1 \ln \frac{y_1}{y_2} dx \right| \\ A_2 &= \left| \int_1^0 \ln \frac{y_1}{y_2} dx \right| \end{aligned} \quad (2.3.10)$$

$$F_{VanNess} = \frac{0.5}{\Delta P\% + \Delta y_1\%} \quad \begin{aligned} \Delta P\% &= \frac{100}{N} \sum_{k=1}^N \frac{|P_k^{exp} - P_k^{calc}|}{P_k^{exp}} \\ \Delta y_1\% &= \frac{100}{N} \sum_{k=1}^N |y_{1,k}^{exp} - y_{1,k}^{calc}| \end{aligned} \quad (2.3.11)$$

$$F_{point} = \frac{1.25}{\delta} \quad \delta = \frac{100}{N} \sum_{k=1}^N \delta_k \quad \delta_k \text{ from eq. (2.3.6)} \quad (2.3.12)$$

$$F_{\infty} = \frac{15}{I_1 + I_2} \quad I_i \text{ from eq. (2.3.7)} \quad (2.3.13)$$

$$F_{pure} = 0.02 / (\Delta P_1^0 + \Delta P_2^0) \quad \Delta P_i^0 = |(P_{i,exp}^{sat} - P_{i,lit}^{sat}) / P_{i,lit}^{sat}| \quad (2.3.14)$$

The maximum value for  $F_l$  is set to 0.25, with the exception of  $F_{pure}$  where the maximum value is preset to 1. If some part of the test is not applicable to the data, then  $F_l = 0.125$  or  $F_{pure} = 0.5$ . Thus the best  $Q$  factor is 1 for a full set of  $xyTP$  data, 0.63 for  $zTP$  data and 0.375 for  $xyT$  data.

## 2.5. Theoretical background of the UNIFAC and COSMO-RS models

One of the hopes of chemical engineers is to establish relatively simple rules that allow for the calculation of the thermodynamic properties of a multicomponent multiphase system from the structure of the constituent chemicals. Models that are based on this principle are called predictive models. The UNIFAC and the COSMO-RS models represent two successful examples of those.

### **2.5.1. UNIFAC (UNIQUAC Functional-group Activity Coefficients) model**

A great advance in development of predictive models was the invention of group contribution methods (GCM). GCMs allow for the prediction of the thermodynamic properties of a system, for which no experimental data are available, by utilizing existing experimental data for other systems. The main principle of the methods is the calculation of the thermodynamic properties of a component or mixture from group contributions. In the UNIFAC activity coefficient model [10], the groups are the functional groups of a molecule. The group contributions for the activity coefficients are optimized based on available experimental equilibrium data. Thus, the UNIFAC model is a semi-empirical model. The UNIQUAC model is a foundation of the UNIFAC model, i.e. the interaction energies of a molecule are calculated based on the surface interactions and the combinatorial contribution to the energy is calculated based on the volume and surface fractions. The main difference between the UNIQUAC and UNIFAC is that in the latter the volume and surface fractions are fractions of the functional group but not the molecules themselves. The UNIFAC group models have been under intensive development since 1975, different functional groups have been defined and their contributions optimized [11-15]. Originally, the VLE data were used for UNIFAC parameter optimization. However, prediction of other thermodynamic properties, such as excess enthalpy ( $h^E$ ), infinite dilution activity coefficients ( $\gamma^\infty$ ) or heat capacity, should also be possible with the activity coefficient models. Thus, improved UNIFAC performance on the  $h^E$  and  $\gamma^\infty$  data was achieved with the modification of the temperature dependency of the group interactions and the modification of the form of the combinatorial part in the UNIFAC-Dortmund model (UNIFD) [16]. The new descriptions required a new optimization of all group contribution parameters. The new model parameters have been published in several articles written by the Dortmund research group [17-22], including parameters for the aromatic sulfur group (ACS, [18]) which were used in this work for calculations of the thiophene – hydrocarbon phase equilibrium.

### **2.5.2. COSMO-RS (COnductor-like Screening Model for Real Solvents)**

A new and interesting theoretical model for the description of molecule interactions was suggested in 1995 by Klamt [23]. The original idea of the author was to quantify real solvation phenomena with the help of quantum chemical methods (QM). The theory is based on continuum solvation

models (CSMs). CSMs describe a molecule in a solution using quantum chemical calculations of the solute molecule surrounded by a dielectric continuum. The boundary conditions for the quantum calculations are made assuming that the molecule is placed in the center of a cavity with a distinct surface. The surrounding media is modeled as a continuum either with a certain dielectric constant (in CSM methods) or with an infinite dielectric constant (in continuum solvation methods COSMO). Thus the molecules are characterized by the screening charge density ( $\sigma$ ) formed on the surface of the cavity by the surrounding conductor.

This QM description of the single molecule, however, does not provide a way to treat bulk liquid effects. For that, the liquid state can be considered as an ensemble of screened molecules, where the molecules are closely packed together and their surrounding cavities are enlarged to minimize the space between the cavities. The interactions between the molecules in this case can be modeled by the interaction of the charged surfaces. Electrostatic and hydrogen bond interactions can be described using the surface effective contact area parameter ( $a_{eff}$ ) and the charge densities of the contacting surface segments ( $\sigma, \sigma'$ ).

$$E_{inter} = a_{eff} \frac{\alpha}{2} (\sigma - \sigma')^2 \quad (2.5.1)$$

$$E_{HB} = c_{HB} \min(0, \sigma_{donor} + \sigma_{HB}) \max(0, \sigma_{acc} - \sigma_{HB}) \quad (2.5.2)$$

The van der Waals interactions can be taken into account using the effective contact area and the element specific adjustable parameters ( $\beta_{vdW}, \beta'_{vdW}$ ):

$$E_{vdW} = a_{eff} (\beta_{vdW} - \beta'_{vdW}) \quad (2.5.3)$$

These microscopic interaction energies  $E_{inter}, E_{HB}, E_{vdW}$  describe the affinity of one surface segment towards another and provide the macroscopic thermodynamic properties of chemical systems with the help of statistical thermodynamics. To achieve that, the partition function ( $Z$ ) of the ensemble of the molecule is to be considered  $Z = Z^C \cdot Z^R$ , where  $Z^C$  is a combinatorial part of the partition function that can be described by the Flory-Huggins expression or by the Staverman-Guggenheim expression [24], as in the COSMO-RS model [25]. The residual partition function  $Z^R$  is defined as

$$Z^R = \sum_p \exp \left\{ -\frac{E}{kT} \right\}, \quad (2.5.4)$$



where  $P$  means samples of all possible pairings of the segments in the ensemble,  $E$  is the total energy of the system sample, and  $k$  is the Boltzmann constant. The total energy is determined by the number of different pair contacts and by the corresponding pair interactions:

$$E(P) = \sum_{\mu\nu} p_{\mu\nu}(P) \varepsilon_{\mu\nu} \quad (2.5.5)$$

where  $p_{\mu\nu}$  is the total number of pairs formed between segments  $\mu$  and  $\nu$  and  $\varepsilon_{\mu\nu}$  is the interaction energy of these pairs [26]. It is extremely complicated to evaluate all the different configurations with respect to the number of pairs of kind  $\mu\nu$ .

Let us assume that the ensemble of molecules in the considered system can be reduced to an ensemble of interacting surfaces. Thus, only the probability distribution of the screening surface charges densities  $\sigma$  (called in COSMO-RS the sigma profile) has to be known for all compounds to describe the composition of the surface segment ensemble.

The residual chemical potential of compound  $i$  ( $\mu_i^R$ ) can be found using equality  $\mu_i = \frac{\partial G}{\partial N_i} = -kT \frac{\partial \ln Z}{\partial N_i}$  and can be written as a sum of the segment chemical potentials  $\mu^\nu$ :

$$\mu_i^R = -kT \frac{\partial \ln Z^R}{\partial N_i} = -kT \sum_\nu \frac{\partial \ln Z^R}{\partial n^\nu} \frac{\partial n^\nu}{\partial N_i} = -kT \sum_\nu \frac{\partial \ln Z^R}{\partial n^\nu} n_i^\nu = -kT \sum_\nu \mu^\nu n_i^\nu \quad (2.5.6)$$

where  $N_i$  is the number of molecules of type  $i$ ,  $n^\nu$  is the number of segments of type  $\nu$ , and  $n^\nu = \sum_i N_i n_i^\nu$ , where  $n_i^\nu$  is the number of segments  $\nu$  in molecule  $i$ .

In publications [25, 27], it was shown that the activity coefficient  $\gamma^\nu$  corresponding to  $\mu^\nu$  ( $kT \ln \gamma^\nu = \mu^\nu - \mu^{\nu\nu}$ ) can be calculated with the following equation:

$$\gamma^\nu = \left( \sum_\mu \Theta^\mu \gamma^\mu \tau_{\mu\nu} \right)^{-1} \quad (2.5.7)$$

where  $\Theta^\mu$  is the fraction of segments  $\mu$  in the solution ( $\Theta^\mu = \frac{n^\mu}{n}$ ),  $\tau_{\mu\nu} = \exp \left\{ -\frac{\varepsilon_{\mu\nu} - \frac{1}{2}(\varepsilon_{\mu\mu} + \varepsilon_{\nu\nu})}{kT} \right\}$  and  $\varepsilon_{ij}$  is the interaction energy between the  $ij$  pair, which is solely dependent on the screening charge density of the interacting surfaces (equations (2.5.1) and (2.5.2)).

It can be shown [26] that equation (2.5.7) corresponds to the pairing function ( $p_{\mu\nu}$ ) that depends not only on the segment total fractions ( $\Theta^\mu$ ,  $\Theta^\nu$ ) as in a random mixing approximation, and on the energy of  $\mu\nu$  pair as in the UNIQUAC model, but  $p_{\mu\nu}$  is also dependent on the activity coefficients of the segments:  $p_{\mu\nu} = \gamma^\mu \Theta^\mu \gamma^\nu \Theta^\nu \tau_{\mu\nu}$ . Equation (2.5.7) can be solved iteratively and provides a

solution for the activity coefficient of the pairwise interacting surface. The solution for the energy calculation of pairwise interacting surfaces was called COSMOSPACE by the authors [25].

Thus through the QM knowledge of molecule screening surface charge densities and with the help of statistical thermodynamics, the chemical potentials of the mixture components can be found. The calculations require some parameterizations: the basic parameters from equations (2.5.1) – (2.5.3) and a few others [28], one from the Staverman-Guggenheim partition function  $Z_{SG}^c$ , two per element of the specific parameters for the vdW interactions ( $\beta$  parameters from eq. (2.5.3)) and one for each element for the cavity radius [28,29]. The optimized parameters are provided by the COSMO-RS model authors in the COSMOtherm software [30]. The program uses the QM calculation file as input information for quick COSMOSPACE thermodynamic calculations. Also, it was recommended [31, 32, 33] that conformations of the molecules have to be considered, because some structures can become more stable due to the presence of solvent.

COSMO-RS has been successfully applied to predict fluid phase equilibria for a variety of chemical engineering applications. An extended potential of the model to calculate VLE has been demonstrated by Spuhl and Arlt [34]. In the present study, COSMO-RS is applied to the systems relevant in gasoline and biofuel production industry.

### 3 Results and discussion

In this chapter the results of publications II – XIII are summarized. The published materials are divided into two groups: experimental results (chapter 3.1, 3.2) and modeling results (chapter 3.3). The measurements and modeling of the molar excess enthalpy are discussed separately in chapter 3.4. A novel approach for improving linearized group contribution methods is presented in chapter 3.5.

Vapor – liquid equilibria measurement techniques and the experimental results are discussed briefly in section 3.1. A summary of the experimental data obtained in publications II – XIII is provided in Table 3.1. The numbers of measured data points of the binary systems, temperature and pressure conditions are shown. Additionally, the quality factor calculated in accordance with recommendations from [8] is given for every measurement. Forty binary systems were investigated in publications II – XIII. Most of the measurements were made isothermally and at a pressure of between 10 and 1700 kPa.

Table 3.1. Summary of the Measured Vapor – Liquid Equilibrium and Excess Enthalpy Data

#	Comp. 1	Comp. 2	Apparatus	Data type	T, K	P, kPa	Points	AZE <sup>a</sup>	Q <sup>b</sup>	Ref	Model used <sup>c</sup>
1	Trans-2-butene	Methanol	Static	<i>zTP</i>	332.1	80.9 - 608	23	+	0.63	IV	LEG5, WIL2, NRTL2, UNIQU2
2		Ethanol				44.8 - 608	24	+	0.63		
3		2-propanol				36.8 - 608	26		0.63		
4		2-butanol				17.3 - 608	24		0.63		
5		2-methyl-2-propanol				36.6 - 608	24		0.63		
6	n-butane	Methanol	Static	<i>zTP</i>	364.5	268.1 - 1440.8	27	+	0.63	V	LEG5-8, WIL2, NRTL2, COSMO-RS, UNIFAC, UNIQ2
7		2-propanol				144.1 - 1284.2	27	-	0.63		
8		1-butanol				36.9 - 1284.8	27	-	0.63		
9		2-butanol				74.2 - 1284.1	27	-	0.63		
10		Tert-butanol				142.6 - 1284.2	27	-	0.63		
11	i-butane	Methanol	Static	<i>zTP</i>	313.05	35.27 - 548.44	24	+	0.62	VII	LEG10, WIL2, UNIQUAC2, NRTL3, UNIFAC, COSMO-RS
12		Ethanol			313.07	17.77 - 531.85	23	+	0.63		
13		2-propanol			313.09	13.77 - 530.75	23	-	0.63		
14		2-butanol			313.06	5.97 - 529.95	25	-	0.63		
15		Tert-butanol			313.08	13.77 - 529.95	26	-	0.63		

#	Comp. 1	Comp. 2	Apparatus	Data type	T, K	P, kPa	Points	$AZ^a$	$Q^b$	Ref	Model used <sup>c</sup>
16	2-propanone	n-butane	Static	$zTP$	364.5	297-1286	26	+	0.63	VI	LEG5, Wil2, UNIQUAC2; COSMO-RS; UNIFAC
17		2-methyl-1-propane			364.1	294-1686	27	-	0.63		
18		1-butene			364.52	297 - 1511	27	-	0.63		
19		2-methyl-propene			365.46	296 - 1546	26	-	0.63		
20		Cis-2-butene			365.46	303 - 1213	27	-	0.63		
21		Trans-2-butene			364.51	297 - 1269	26	-	0.63		
22	MIBK	2-butanol	Circ. HS <sup>c</sup> HE	$xyTP$ $xyT$ $Th^E$	368.2 368.2 297.84	53 - 85 - -	19 11 10	- - -	0.69 0.27 32.9 J/mol	III	Wil6
23	MIBK	Tert-pentanol	Circ. HS Calorim.	$xyTP$ $xyT$ $Th^E$	368.05 368.2 333.2 294.2 297.84	1.65 - 85.35 - -	25 35 14 11 10	- - - + -	0.79 0.35 0.27 0.38 4.2 J/mol	III	
24	MIBK	2-ethyl-1-hexanol	Circ. Calorim.	$xyTP$ $Th^E$	388.2 297.84	8.8 - 93.25 -	20 10	- -	0.52 4.6 J/mol	III	
25	Toluene	Diethyl sulfide	Circ.	$xyTP$	361 - 379.5	90.03	19	-	0.88	VIII	
26		1-propane-thiol			337-379.4		22	-	0.79		
27		thiophene			353 - 379.4		22	-	0.81		
28	Diethyl-sulfide	n-hexane	Circ.	$xyTP$	323.15; 338.15	23.76 - 90.46	36	-	0.93; 1	IX	Wil6, UNIFAC, COSMO-RS
29		1-hexene			323.15; 333.15	23.76 - 90.85	34	-	0.87; 0.97		
30		Heptane			353.15; 363.15	57.34 - 97.4	41	+	1; 0.91	X	
31		Isooctane			353.15; 363.15	57.11 - 97.49	34	+	1; 1		
32		Cyclohexane			343.15; 353.15	50.14 - 99.41	30	-	0.96; 0.94	XI	
33		ETBE			333.15; 343.15	34.97 - 92.96	28	-	0.98; 0.93		
34	Thiophene	n-hexane	Circ.	$xyTP$	323.15; 338.15	31 - 90.4	49	+	0.96; 0.95	IX	Wil2, UNIFAC, UNIFD, COSMO-RS
35		1-hexene			323.15; 333.15	31 - 90.9	34	-	1; 1		
36		Isooctane			343.15; 353.15	41 - 93	37	+	0.9; 0.93		
37		ETBE			333.15; 343.15	45 - 93	35	-	1; 1		

#	Comp. 1	Comp. 2	Apparatus	Data type	T, K	P, kPa	Points	AZE <sup>a</sup>		Ref	Model used <sup>c</sup>
								$Q^b$			
38	Furfural	MIBK	Circ.	$xyTP$	353.3	16 - 32	9	-	0.98	XI	NRTL4, UNIQUAC4, Wil4, LEG4, COSMO-RS, UNIFD
			Static	$zTP$	345.8	4 - 23	14	-	0.48		
			HS	$xyT$	368.5	-	11	-	0.34		
					333.3	-	11	-	0.34		
		Calorim.	$Th^E$	298.15	-	9	-	1.8%			
39	Furfural	2-butanol	Circ.	$xyTP$	353.2	6 - 47	10	-	0.84		
			Static	$zTP$	345.7	4 - 33	14	-	0.63		
			HS	$xyT$	333.3	-	15	-	0.37		
		Calorim.	$Th^E$	298.15	-	9	-	2.8%			
40	Furfural	Tert-pentanol	Circ.	$xyTP$	353.2	6 - 43	14	-	0.89		
			Static	$zTP$	345.6	4 - 31	15	-	0.63		
			HS	$xyT$	333.3	-	11	-	0.35		
		Calorim.	$Th^E$	298.15	-	16	-	1.5%			

<sup>a</sup> Azeotrope; <sup>b</sup>  $Q$  is the quality factor; <sup>c</sup> LEG5 or LEG4 is the Legendre polynomial with 5 or 4 parameters correspondingly [9], NRTL2 or NRTL4 are NRTL models with 2 or 4 parameters correspondingly [35], UNIQUAC2 or UNIQUAC4 are UNIQUAC models with 2 or 4 parameters correspondingly [36], Wil2, Wil4 or Wil6 are Wilson models with 2, 4 or 6 parameters correspondingly [37], UNIFD is the UNIFAC-Dortmund model [38], COSMO-RS is a conductor-like screening model for a real solvent [23] as implemented in COSMOtherm software; <sup>c</sup> HS is headspace gas chromatography [39]

### 3.1 Experimental measurements

Two of the most important separation techniques in the modern chemical industry are distillation and extraction. Solid - liquid and liquid – liquid extractions are widely used for the separation of chemical compounds, but the most used method in the chemical industry is a distillation. Vapor – liquid equilibrium (VLE) measurements provide the information required for the design and operation of distillation and extraction columns. Numerous techniques exist for measuring VLE. In publications II-XIII, static total pressure apparatus, recirculation still apparatus, and headspace gas chromatography were used for the VLE measurements.

#### 3.1.1 Static total pressure apparatus

A schematic diagram of the static total pressure apparatus is shown in Figure 3.1.1. The apparatus is also described in detail in [40] and publications IV – VII.

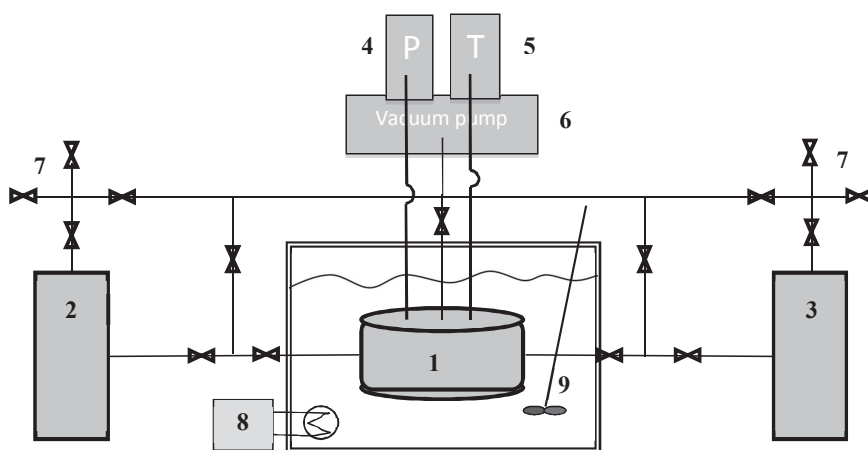


Figure 3.1.1. Static total pressure apparatus. (1) equilibrium cell equipped with mixer, (2) and (3) ISCO syringe pumps equipped with temperature control systems and temperature probes, (4) pressure display and pressure transducer equipped with temperature control system and temperature probe, (5) cell temperature probe, (6) vacuum pump, (7) feed and vacuum lines, (8) temperature control unit, (9) mixer.

The measurements taken by the static apparatus are based on recordings of the total pressure of cell (1) with pressure transducer (4) at constant temperature controlled by thermostat (8). Syringe pumps (2,3) inject the preset volume of the chemical into the cell. The temperature, pressure, and volume of the pumps are recorded for the recalculation of the molar amount of the chemicals loaded into the cell.

The measurement starts with an injection of pure compound from syringe pumps (2,3) into the vacuumed cell (1) and recording of the system pressure. Before the measurements the liquids are degassed. If the measured pressure does not change with the addition of the first component, the second component is added stepwise into the cell until an approximately equimolar composition is achieved. Cell pressure is recorded at each step. The procedure is repeated starting from the measurement of the pressure of the pure second component. Overlapping of the measured pressure lines around the equimolar composition indicate good quality of the measured data and sufficient degassing of the pure compounds.

### 3.1.2 Reduction of the static total pressure apparatus data

In the static total pressure experiments, only the pressure and temperature are measured directly. The overall system composition ( $z$ ) is calculated based on the amount of chemical loaded into the cell by the syringe pumps. The initial composition, pressure, and temperature define the distribution of the binary system components between phases. The phase compositions, however, depend on the fugacity and activity coefficients, which in turn depend on the compositions. Thus, an iterative procedure for the search for phase compositions and activity coefficients was proposed by Barker [41]. This approach assumes that we know the form of the dependency between the activity coefficients and composition, i.e. the activity coefficient model for the calculations is preselected. This assumption results in a priori thermodynamic consistency of the data obtained with the Barker regression when consistent  $G^E$  models are used. The quality of the regressed data can be checked only using the Van Ness consistency test and by comparison of the pure compound pressures with the literature values. The Barker procedure was used in all the publications of our group with static apparatus measurements, including publications IV – VII and II.

The total cell composition is calculated with the volume of the components introduced by the syringe pumps at the temperature and pressure of the pumps. For precise recalculation of the component molar amounts from the injected volumes, the density correlation for each component is required. Moreover, the density should be available for the temperatures and pressures of the syringe pumps. In publications IV – VII and II, the literature density correlations were utilized [42], [43]. The dependency of density on pressure was estimated with the Hankinson-Brost-Thomson correlation [44] and with the vapor pressure correlations of pure compounds taken from the literature [45].

### 3.1.3 Uncertainty of the static total pressure apparatus data

Only a few experimental variables are actually measured in the static apparatus experiments. The syringe pump parameters are temperature, pressure, and volumes of the injected component ( $T_{pump}, P_{pump}, \Delta V_{i, i=1, m}$ ), and the cell parameters are temperature, pressure, and the cell total volume ( $T_{cell}, P_{cell}, V_{cell}$ ). The standard deviations of these parameters were estimated from the calibration of the equipment.

These experimental variables and the literature correlation are used together for the recalculation of the phase compositions as shown in Figure 3.1.2, where  $\overline{PAR}$  denotes the vector of the activity coefficient model parameters,  $n_i$  is the molar amount of injected component  $i$  and  $z_i$  is the total cell composition with regard to component  $i$ :

$$\begin{aligned}
x_i &= x_i(T_{cell}, P_{cell}, n_{i,i=1,m}, V_{cell}, \gamma_{i,i=1,m}) & \gamma_i &= \gamma_i(T_{cell}, P_{cell}, x, y, V_{cell}, \overline{P\overline{A}R}) \quad (3.1.1) \\
y_i &= y_i(T_{cell}, P_{cell}, n_{i,i=1,m}, V_{cell}, \gamma_{i,i=1,m}) \\
n_i &= n_i(\rho_i(T_{i,pump}, P_{i,pump}), \Delta V_i) \quad (3.1.2) \\
\rho_i &= \rho_i(T_{i,pump}, P_{i,pump}) \quad (3.1.3) \\
z_i &= z_i(n_{i,i=1,m}) \quad (3.1.4)
\end{aligned}$$

Figure 3.1.2. Uncertainty estimation schema for the static total pressure data.

In accordance with the error propagation theory proposed by Taylor [46], the uncertainty of a calculated variable ( $M$ ) can be estimated using a derivative of the variable with respect to all the measured variables ( $x_1, x_2, \dots, x_n$ ), if the measured variables are independent and their errors are randomly distributed:

$$\delta M(x_1, x_2 \dots x_n) \leq \left| \frac{\partial M}{\partial x_1} \right| \delta x_1 + \left| \frac{\partial M}{\partial x_2} \right| \delta x_2 + \dots + \left| \frac{\partial M}{\partial x_n} \right| \delta x_n \quad (3.1.5)$$

The uncertainty of density eq. (3.1.3) is estimated with derivatives of density regarding pump temperature and pressure ( $T_{pump}$ ,  $P_{pump}$ ). The derivative of density in respect of temperature is calculated using the  $\rho - T$  correlation from the literature [42], and the derivative of density with respect to pressure is calculated from the Hankinson-Brobst-Thomson correlation [44].

The uncertainty of the molar amount of injected components ( $n_i$ ) is calculated by differentiating equation (3.1.2) with respect to density function (3.1.3) and with respect to injected volumes (see publication IV and [47]). The standard uncertainty of  $\rho_i$  is taken from the literature and that of  $\Delta V_i$  is estimated from the syringe pump calibration.

The uncertainty of the total cell composition ( $z$ ) is calculated based on the analytical derivative of equation (3.1.4) [48] considering  $z$  as a function of  $n_i$ , which in turn depends on  $\rho_i$ , and  $\Delta V_i$  eq.(3.1.2). Thus the  $\Delta z_i$  value can be calculated analytically using standard deviations of measured and literature values  $\Delta \rho_i$ ,  $\Delta V_i$ ,  $\Delta T_{i,pump}$  and  $\Delta P_{i,pump}$ .

The calculation of mole fractions ( $x_i, y_i$ ) and activity coefficients ( $\gamma_i$ ) requires an iterative procedure (see chapter 3.1.2). The maximum errors of the variables were calculated by performing the Barker reduction using the lower and upper boundary of  $T_{cell}$ ,  $P_{cell}$  and  $n_i$  and selecting the maximum deviation from the results of the original Barker reduction as an estimation of the reduced variable uncertainty. It should be noted that the maximum of the variable deviations does not necessarily occur at the lower or upper boundaries of the measured variables.



### 3.1.4 Results of the static total pressure apparatus data

The static total pressure apparatus was used in publications IV – VII and II for the measurements of twenty-four binary systems. In publications IV, V and VII the alcohol-containing binaries were measured in mixtures with trans-2-butene, n-butane and i-butane. In publication VI, the VLE of the systems containing 2-propanone was investigated. In these systems, the range of the operating pressure was very wide, from tens to thousands of kilopascals. During the work for publication II, the static apparatus was used in a low pressure range (from 4 to 33 kPa), see Figure 3.1.3.

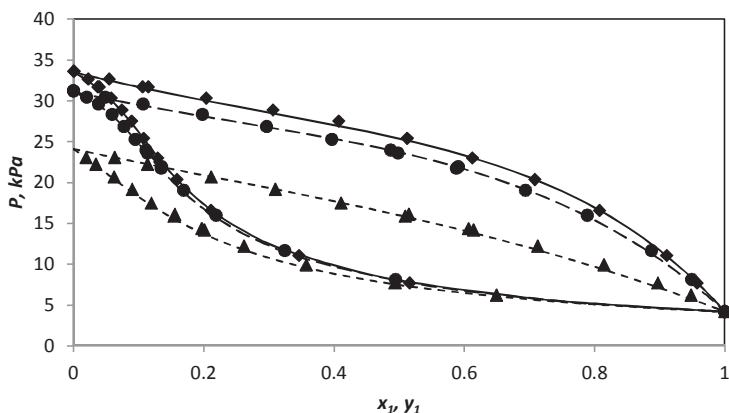


Figure 3.1.3. Pressure – composition diagram measured at static total pressure apparatus for furfural-containing systems at 346 K; (♦) with 2-butanol, (▲) with MIBK, (●) with tert-pentanol; (—), (---), (— · —) corresponding NRTL models.

All the measured binaries exhibited a positive deviation from Raoult's Law and a moderate range of activity coefficients, see Figure 3.1.4. The highest activity coefficients (up to 45 in the infinite dilution range) were observed for i-butane systems with methanol and ethanol and in mixtures of methanol with n-butane and trans-2-butene. In these same systems, azeotropic behavior was observed.

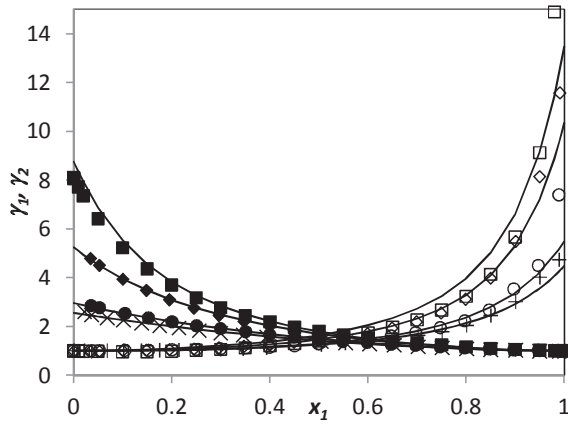


Figure 3.1.4. Activity coefficients calculated by means of Barker regression on the static total pressure data for systems containing trans-2-butene at 326 K, (■) trans-2-butene (1) + (□) methanol (2) activity coefficients; (◆) trans-2-butene (1) + (◇) ethanol (2) activity coefficients; (●) trans-2-butene (1) + (○) 2-butanol; (×) trans-2-butene (1) + (+) TBA; (—) NRTL model.

The obtained data are of good quality (Table 3.1). The Van Ness consistency test, a test for the capability of a model to reproduce measured data, showed that the data are of the best possible quality for that type of measurement (*zTP* measurements), i.e. 0.63 (see also chapter 2.3).

### 3.1.5 Recirculation still apparatus

A simplified schematic diagram of the recirculation still apparatus used in publications II - III, VIII – XIII is shown in Figure 3.1.5. This Yerazunis-type recirculation still apparatus [49] was described in detail in [50] and in publication XIII.

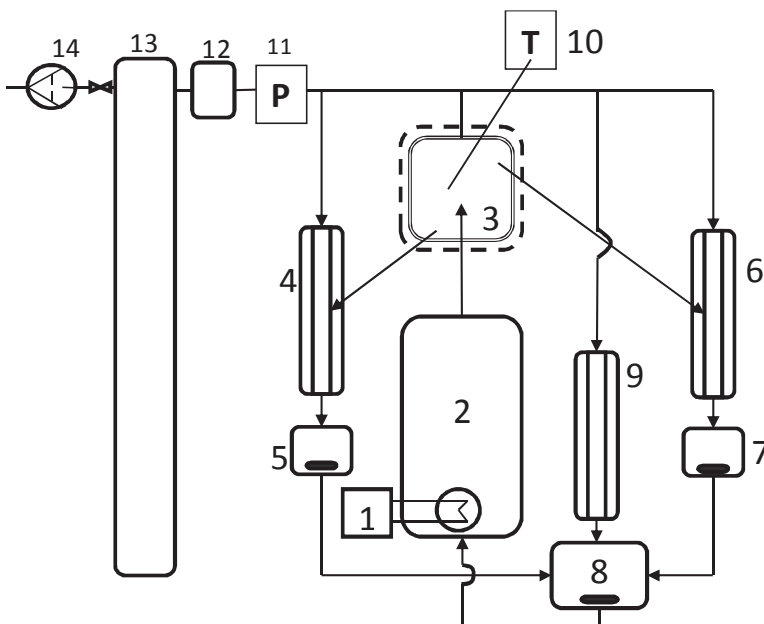


Figure 3.1.5. Schematic diagram of the recirculation still apparatus. (1) heater, (2) boiling chamber, (3) equilibrium cell, (4), (6), and (9) condensers, (5) and (7) sampling chambers with stirrers, (8) mixing chamber with stirrer, (10) temperature probe, (11) pressure transducer and indicator, (12) liquid nitrogen trap, (13) buffer tank, (14) rotary vane vacuum pump.

Liquid of a certain composition is boiled in chamber (2). In equilibrium chamber (3), the boiled stream splits into liquid and vapor and the flows pass into condensers (4) and (6). The sampling of the vapor and liquid phases is done after stabilization of the temperature and pressure through the sampling chamber septa by means of syringes. The condensed vapor and liquid flows are combined in mixing chamber (8) and recirculated to the boiler. The condensers, equilibrium cell, and mixing chamber are connected to the pressure control system: pressure transducer and indicator (11), liquid nitrogen trap (12), buffer tank (13) and vacuum pump (14). As the equipment is made of glass, only atmospheric and sub-atmospheric pressures can be measured in the apparatus. Buffer tank (13) of about 30 liters in volume is used between the vacuum pump and the apparatus for

stabilization of the system pressure. The overall load of the chemical in the recirculation still apparatus is about 80 cm<sup>3</sup>. A change in boiling mixture composition is done by withdrawing the liquid or vapor phase and adding one of the components of the binary mixture into the apparatus. The important part of recirculation still measurements is the composition analysis of both liquid and vapor phases. This can be considered a disadvantage if the composition analysis of the mixture is challenging. On the other hand, the recirculation measurements provide a full set of experimental VLE information ( $xyTP$ ) and the consistency of the data can be checked.

In publications II – III and VIII – XIII, gas chromatography (GC) analysis was used for determining the phase compositions, and in publications III, X and XIII, the analysis was duplicated by determining the composition with a refractometer.

### **3.1.6 Uncertainty of the recirculation still data**

In the recirculation still, the uncertainties of temperature and pressure were estimated either with the uncertainty specified by manufacturers of temperature and pressure sensors, or were estimated using the calibrations. These are provided in publications II, III, VIII – XIII. The uncertainties of the GC compositions were estimated based on the calibration of the GC FID detector on gravimetrically prepared liquid samples. The uncertainty of the activity coefficients was calculated with the derivative of equation (2.1.5) with respect to temperature, pressure and phase compositions. Uncertainties of vapor pressure correlation or the Rackett equation of state [6] were not taken into account and are considered to be minor.

### **3.1.7 Results of the recirculation still data**

Overall nineteen binary systems were measured with the recirculation still apparatus: binaries containing MIBK, furfural, diethyl sulfide and thiophene (Figures 3.1.6-7, and the figures in sections 3.4.5 – 3.4.7). All the investigated systems showed positive deviations from Raoult's Law. The activity coefficients were below two in systems containing MIBK, thiophene and diethyl sulfide, and below four for the furfural systems. The maximum pressure azeotropes were found in the thiophene + isooctane, thiophene + n-hexane, diethyl sulfide + n-heptane, and diethyl sulfide + isooctane systems.

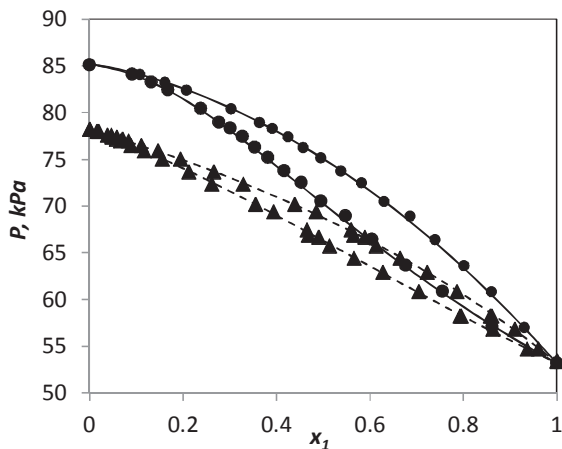


Figure 3.1.6. Pressure composition diagram for the binary system containing MIBK: (●) experimental points for MIBK (1) + 2-butanol (2), (—) NRTL model; (▲) experimental points for MIBK (1) + tert-pentanol (2), (- -) NRTL model.

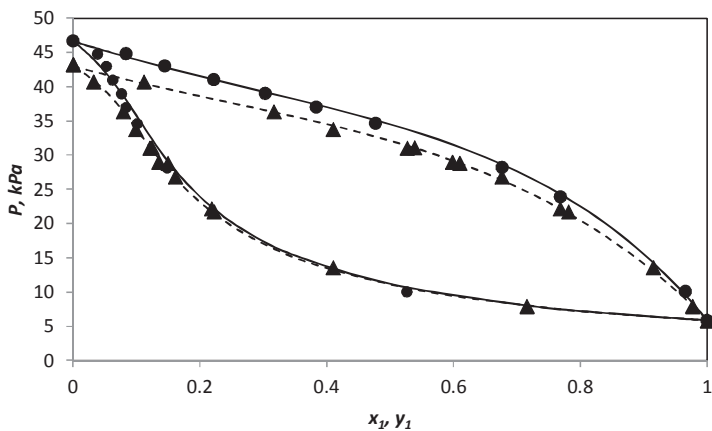


Figure 3.1.7. Pressure composition diagram at 353.2 K (●) furfural (1) + 2-butanol (2) system experimental points and (—) NRTL model; (▲) furfural (1) + tert-pentanol (2) system experimental points and (- -) NRTL model.

The consistency of the data was checked with four different tests for all the investigated binary systems (the area, Van Ness, point, and infinite dilutions tests, see section 2.3). The area test was passed in most of the experiments. In MIBK + alcohol, the quality factor was rather low (from 0.5 to 0.8 from a maximum of 1). These system activity coefficients were close to one over the whole

range of concentrations; this caused high deviations in the area and infinite dilution tests and thus a reduction of the quality factor. All VLE data measured for sulfur-containing compounds in the recirculation still apparatus are of very good quality (with a quality factor  $Q \geq 0.8$ ). The lowering of the quality factor arises mainly from the comparison of the measured pure compound pressure with the literature value. Deviation of the literature vapor pressure from measured by 5% may reduce the quality factor down to 0.27. In all the calculations, the DIPPR database vapor pressure [43] was used as a reference. In sulfur- and MIBK- containing systems, the discrepancy between measured and literature pure compounds pressure was from 0.5 to 2% that cause some quality factor reduction but in most cases the quality factor was higher than 0.7. For furfural-containing systems, the main reason for the data quality reduction was the high residual between that predicted by the model and the experimental mixture pressure (the Van Ness test). The data of four different techniques included in the optimization of model parameters (NRTL, UNIQUAC, Wilson) were difficult to model with 1% accuracy for the furfural-containing systems.

### 3.1.8 Headspace gas chromatography (HS)

HS is a gas chromatography technique complemented by a gas phase sampling apparatus. The gas sampler takes a vapor sample from the headspace of the vial and injects it into the gas chromatograph column. Several versions of the vapor sampling technique exist. In most commercial headspace sampling equipment, two main vapor-sampling methods are utilized, i.e. the automated balance pressure method and the pressure/loop method [39]. In the latter, the sample is transferred first to the sampling loop and then injected into the column, whereas in the automated balance pressure method, the vapor sample is injected directly from the vial headspace into the column. In publications II and III, a pressure/loop vapor sampler was used (Agilent Technology Headspace sampler 7697A). The three stages of vapor sampling are shown schematically in Figure 3.1.8.

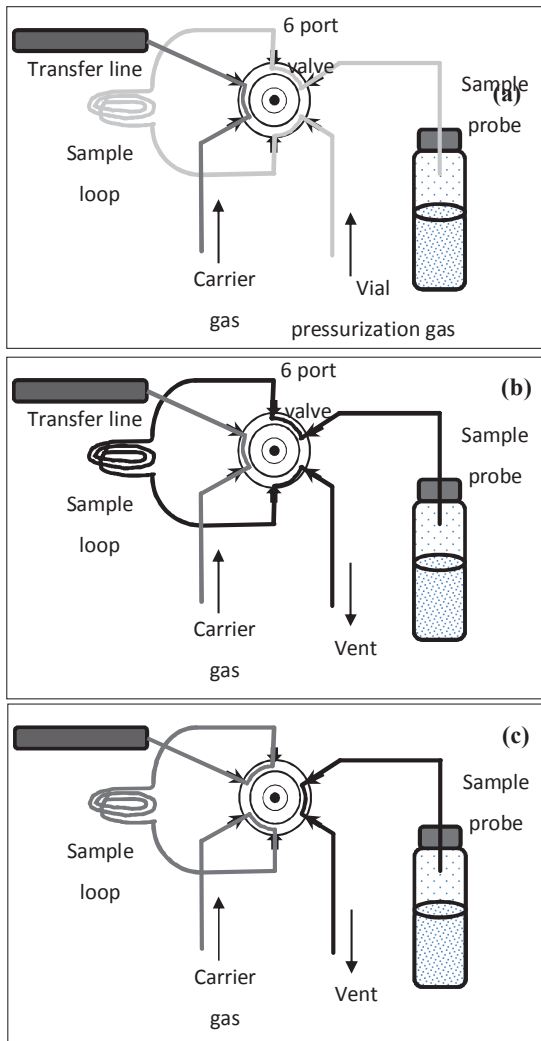


Figure 3.1.8. Three stages of vapor sampling with the pressure/loop system; the schematic figures are based on figures provided in [51]: (a) vial pressurization stage, (b) sample loop filling stage, (c) injection stage.

Vapor sampling for the pressure/loop system is done by means of a 6-port valve. In stage (a) (Figure 3.1.8) the vial is pressurized with an inert gas ( $N_2$  or He). In stage (b), the vial is connected to the loop and the loop is filled by purging, and finally, in stage (c), the loop is connected to the column and the sample is transferred into the column by the carrier gas. For VLE measurements with the HS technique, sampling should be done in such a way that it does not disturb the

equilibrium in the vial. The formation of cold spots on the route of the sample into the column should be avoided to prevent condensation of components. The amount of the vapor sample should be large enough to be detectable by GC. The main control parameters of the sampling process are vial pressurization pressure, pressurization time, loop volume, loop filling pressure, and column carrier gas pressure. The operating parameters for HS measurements were optimized and are provided in publications II and III.

### 3.1.9 Reduction of headspace gas chromatographic data

Headspace gas chromatography (HS) requires data reduction. Only the gas phase composition and temperature are measured experimentally in HS measurement. The pressure is not measurable with this type of technique, as the vial gas phase contains air. The vial liquid phases were prepared gravimetrically and consequently, the initial liquid compositions are known with good accuracy. However, the composition of the liquid phase is changed with the formation of the gas phase above the liquid. This compositional change can be calculated if the activity coefficient of the new liquid phase is known. Therefore, the iterative determination of the liquid composition is needed. This procedure is described in [52]. However, iterations for the correction of the liquid composition were not used, because the change of the activity coefficient for the system under investigation was negligible within the change of liquid composition. Thus, the concentration change was calculated, taking into account the activity coefficient estimated by the UNIFAC-Dortmund (UNIFD) activity coefficient model for the initial liquid composition. Assuming ideal vapor behavior ( $PV=nRT$ ;  $\phi_i, \phi_i^0 = 1$  in eq. (2.1.5)) and neglecting the Poynting correction, the equation for the liquid composition correction becomes

$$\Delta x_i = x_{i,0} - \frac{n_{i,0} - n_i^V}{\sum_j n_{j,0} - n_j^V}, \text{ where } n_i^V = \frac{y_i x_i P_i^{sat} V}{RT} \quad (3.1.6)$$

The formation of the vapor phase did not change the liquid phase composition considerably due to the small size of the vapor sample, the large difference in the phase densities. Usually, the liquid composition change is in the third decimal of a molar fraction of the liquid composition or smaller, thus the correction of the liquid composition is important only for low component concentrations.

The activity coefficients of the components in HS measurement can be calculated using the following expression [53]:

$$\ln \frac{y_1}{y_2} = \ln \frac{y_1 x_2 P_2^{sat}}{y_2 x_1 P_1^{sat}} \quad (3.1.7)$$



### 3.1.10 Uncertainty of headspace gas chromatographic data

The temperature uncertainty for the HS data was estimated by calibrating the HS oven against the certified temperature sensor. The accuracy of the temperature measurement was found to be comparable with the standard error stated by the equipment manufacturer. The uncertainty of the liquid phase composition consists of the uncertainty of the gravimetric preparation of the liquid samples and the uncertainty related to formation of the vapor phase. The former was estimated as a balance uncertainty. Uncertainty caused by correction of the liquid composition was not taken into account. This uncertainty is negligible, because the mole number of the compounds in the vapor phase is relatively small in comparison with the liquid mole numbers (a ratio of about 1:100) and the change of the vapor molar composition with a small variation of temperature is even less. The vapor phase composition uncertainty was estimated based on the GC FID calibration.

### 3.1.11 Results of headspace gas chromatographic data

The VLE of five binary systems was measured by the HS technique: MIBK + 2-butanol, MIBK + tert-pentanol, furfural + MIBK, furfural + 2-butanol and furfural + tert-pentanol as described in publications II and III. Some of the measurements were repetitions of the VLE data available from the literature or from measurements made with a recirculation still apparatus (MIBK + 2-butanol, furfural + MIBK). This allowed us to adjust the parameters of vapor sampling and verify the applicability of the optimized HS method for the VLE measurements under consideration. The investigated VLE measurements were also made at low temperatures (333 and 298 K). At these temperatures, the uncertainty of the system pressure measurement of the MIBK- and furfural-containing systems was too high for the pressure sensor of the static pressure or recirculation still apparatus used in our laboratory. In our HS measurement, a low pressure is not an obstacle as long as the mixture components are detectable by GC at the experimental conditions. The composition diagram for MIBK + tert-pentanol at different temperatures is shown in Figure 3.1.9 (a). This system exhibits azeotropic behavior. The VLE diagram for furfural-containing systems at 333.3 K is presented in Figure 3.1.9 (b). It can be seen that, in the MIBK-containing systems, the compositions of vapor and liquid phases are close to each other, whereas for furfural-containing systems, the furfural concentration in the vapor phase is much lower than in the liquid phase.

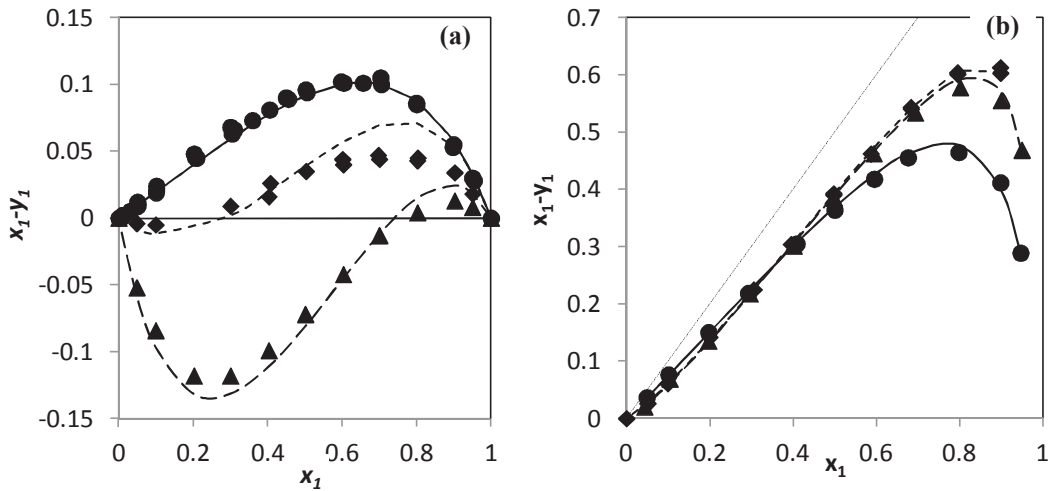


Figure 3.1.9. Composition diagram of VLE HS measurements for (a) MIBK (1) + tert-pentanol system (●) experimental points and (—) NRTL model at 368.2 K, (◆) experimental points and (- -) NRTL model at 333 K, (▲) experimental points and (—) NRTL model at 294 K; (b) furfural- containing systems at 333.3 K (●) furfural (1) + MIBK (2) experimental points and (—) NRTL model, (◆) furfural (1) + 2-butanol experimental points and (- -) NRTL model, (▲) furfural (1) + tert-pentanol (2) experimental points and (—) NRTL model; (⋯)  $y_1 = 0$  line.

The measured HS data complement the measurements made with other experimental apparatus and increase the range of applicability of the activity coefficient model parameters fitted with the data. However, HS data provide only  $xyT$  experimental variables, which do not allow us to perform most of the consistency tests. Thus the quality of HS data is often uncertain, which is reflected in the low maximum quality factor for HS data (0.38).

The HS experiments published in publications II and III have a quality factor from 0.27 to 0.37. For furfural-containing systems, the reduction in the quality was related to the deviation between the experimental data and the prediction of the model which was optimized with four different sets of binary data (the Van Ness consistency test). For the MIBK-containing binary systems, the reduction of the quality factor is due to the area test, which is not informative for systems close to ideal [8]. Moreover, additional consistency deviation can be introduced by using pressure correlation from the literature in the HS data area test calculations (see eq. (3.1.7)). An increase of as much as 50% in the consistency parameter ( $D$ , see eq.(2.3.10)) is possible due to a 5% error in the vapor pressure correlation in systems close to ideal.

The HS results obtained in this work were used for extending the optimized NRTL, UNIQUAC and Wilson models for temperature, where other experimental techniques are not suitable for VLE measurements. However, the VLE HS data obtained in publications II or III cannot be used alone for reliable fitting of thermodynamic model parameters due to the scattering of the HS data. This scattering was caused by instability in the vapor sampling.

### 3.1.12 Calorimetry

Excess enthalpy was measured in publications II and III for furfural- or MIBK-containing systems with a SETARAM C80 flow calorimeter. The principal diagram of the apparatus is shown in Figure 3.1.10.

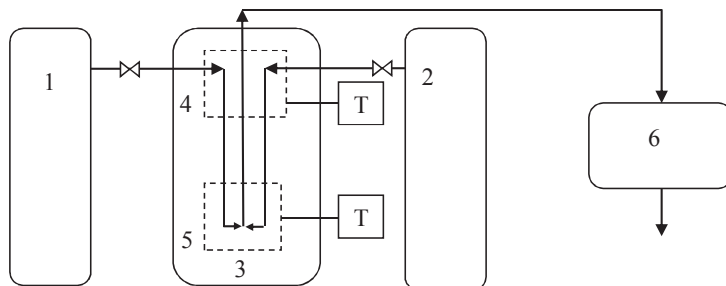


Figure 3.1.10. Schematic diagram of the excess enthalpy measurement system. Syringe pumps (1) and (2) equipped with a temperature control system, (3) SETARAM C80 calorimeter, (4) preheater with a temperature probe, (5) flow mixing cell with a temperature probe, (6) DMA 512P densimeter equipped a temperature control system.

The component flow is provided by syringe pumps (1) and (2) with thermostats. In calorimeter (3) the flows are preheated and mixed in flow mixing cell (5). Heat release is recorded together with temperatures in the mixing area and in the preheating area. After the calorimetric measurement, the mixed flow that is formed can be used for density measurements. The calorimeter was calibrated on cyclohexane + hexane and methanol + water binary systems, as recommended in [54].

### 3.1.13 Uncertainty of calorimetric measurements

The calculation of the molar fraction of the calorimetric measurements is done using the volumetric flows of the syringe pumps, their temperatures, and DIPPR density correlations [43]. The uncertainty of the mole fraction is calculated from the derivative of the equation for the mole fraction with respect to molar flow. The molar flow is a function of the volumetric flow of the

syringe pump. The standard deviation of the volume measurement of the syringe pump is found experimentally by pump calibration. The uncertainty of the molar excess enthalpy is taken as 1.3% of the measured value in accordance with the accuracy of the equipment specified by the manufacturer.

### 3.1.14 Results of the calorimetric measurements

The molar excess enthalpies were determined for MIBK- and furfural-containing systems in publications II and III. The measured molar excess enthalpies of the systems were highly positive (see Figure 3.1.11), i.e. above  $1300 \text{ J}\cdot\text{mol}^{-1}$ . The highest molar excess enthalpy was observed in mixtures with 2-butanol for both MIBK- and furfural-containing systems. For the MIBK + furfural binary system, the molar excess enthalpy was  $247 \text{ J}\cdot\text{mol}^{-1}$  at maximum. The obtained  $h^E$  data were combined with VLE data to fit the parameters of the activity coefficient models (NRTL, UNIQUAC and Wilson). Additional temperature dependence was required for the simultaneous description of  $h^E$  and VLE data. Thus, experiments at different temperatures are needed for setting up a reliable model of these systems in a wide range of temperatures. The temperature of the VLE measurements was limited by minimum operation pressure of measurement technique, so the excess enthalpy measurements were very useful for extending the model applicability to other (lower) temperatures.

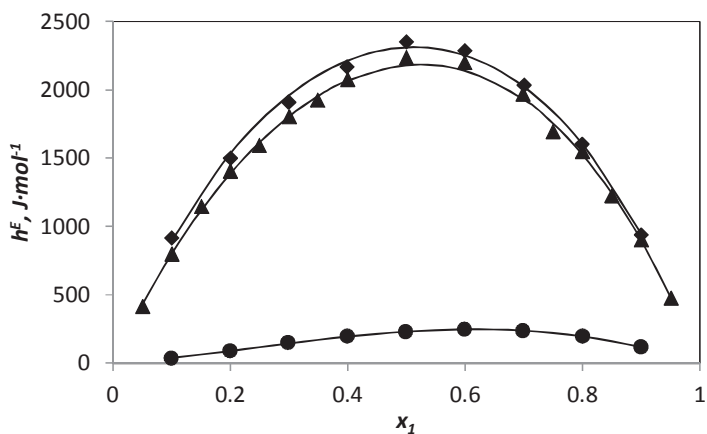


Figure 3.1.11. Molar excess enthalpy for furfural-containing systems at 298 K: (●) furfural (1) + MIBK (2) experimental points and (—) NRTL model, (◆) furfural (1) + 2-butanol (2) experimental points and (—) NRTL model, (▲) furfural (1) + tert-pentanol (2) experimental points and (—) NRTL model.

### 3.1.15 Gas chromatography

Gas chromatography was used for the analysis of liquid and vapor phase compositions in publications II – XIII. HP 6850A and Agilent 6890N gas chromatographs were equipped with nonpolar HP-1, slightly polar HP-1701, and polar DB-WaxETR capillary columns. The GC inlet, GC detector, and GC oven operation regimes were adjusted for the separation and reliable detection of the mixture compounds, as specified in publications II, III, VIII - XIII. The GC FID detector was calibrated against gravimetrically prepared standard solutions of the binary mixtures. The same calibrations were used in the determination of the vapor phase compositions. The main difference between the vapor and liquid sample analysis was the smaller GC injector split ratio employed for the vapor phase samples, because of the smaller amount of chemical per injection in the vapor samples. For some measured binary systems, the GC analysis was verified by refractive index measurements.

### 3.2 Comparison of measurement techniques used

Several experimental techniques were used in this thesis for measuring the VLE and  $h^E$  of normal hydrocarbons, alcohols, sulfur-containing compounds, ketones, and furfural.

In Table 3.2., the measurement techniques used in this work are compared.

Table 3.2. Comparison of the measurement techniques used in this work.

	Static	Recirculation	HS	Flow calorimetry
T range, °C	0 – 90 (200)	25 – 150 (200)	25 - 230	25 – 50 (300)
P range, kPa	1 – 5000	20 – 100	Volatile comp.	-
Data type	$zTP$	$xyTP$	$(x)yT$	$xh^E$
Quality factor	0.63	1	0.38	-
Possibility to automate	+	-	+	+
Analysis of components	-	+	partly	-
Time per binary system	2-3 days	3-5 days	2-3 days	2-3 days

As can be seen, the static apparatus has the widest range of operational pressure, though the data it produces does not include liquid and vapor compositions. The maximum quality factor for the data (see chapter 2.3) is only 0.63 out of a maximum of 1. The measurement procedure can be automated [IV] and the measurement time for one binary VLE is about three working days. The technique is not recommended for measuring potentially reacting compounds, as the presence of the reaction products is not checked. The recirculation still apparatus is more suitable for mixtures that are likely to undergo side reactions, because the composition of the phases is analyzed. The technique provides a full set of data ( $xyTP$ ). The temperature and pressure operation range is limited for this technique and its accuracy may be low for binary systems with a large difference

in the boiling point of the components [50]. Headspace gas chromatography is automated and a fast measurement technique that can be applied to relatively volatile compounds ( $P^{sat}$  at  $T^{meas} \geq 1$  kPa). However, only gas composition and temperature is measured experimentally in this technique. Additional measurement time is required for the adjustment of vapor sampling regimes and repetition of experiments to compensate the vapor-sampling scattering. Calorimetry with the flow-mixing cell does not provide equilibrium data, but allows the extension of measured VLE data to other temperatures. In this respect, the technique is a good choice for nonreactive systems in addition to VLE measurement.

### 3.3 Optimization of the Activity coefficient model parameters

Data obtained in publications II – XIII were used for optimization of the activity coefficient model parameters (Wilson, NRTL, UNIQUAC). Objective function for the optimization depended on the data source. Thus, with excess enthalpy data the relative absolute error of excess enthalpy was used as a summand of the objective function for the minimization. With the HS data the relative absolute error of vapor composition was a summand, and the relative absolute error of pressure was a summand for the static total pressure and the recirculation still data. The sum of the errors was minimized in two steps [55]. At first the algorithm of Nelder and Mead [56] finds a minimum and then the Davidon optimization [57] refines the minimum.

As can be seen from chapter 2.2, the level of complexity of excess Gibbs energy description increases from the Wilson to the NRTL and the UNIQUAC models. However, for the systems considered in publications II – XIII these models had comparable accuracy regarding the description of the VLE data. It appears that the components of the investigated binary systems were of similar size. The temperature dependence of the interaction parameters of the models ( $\Lambda$ ,  $\tau$ ) was often utilized. The additional temperature-dependent parameters increased the flexibility of the models. Thus, even a relatively simple Wilson model was able to reproduce the experimental data. As expected, the accuracy of the model correlations of the measured binary system VLE was always better in comparison with the accuracy of the predictive models (see below, chapter 3.4).

### 3.4 Prediction of VLE with UNIFD and COSMO-RS predictive models

This part of the thesis summarizes the comparison of two predictive models (UNIFD and COSMO-RS) for their ability to predict the measured VLE data. The comparison is based on the new experimental data published in articles II – XIII and will show some pros and cons of the predictive models. However, general conclusions will not be drawn about the predictive abilities of the UNIFD and COSMO-RS models because of the relatively small amount of data considered. The data used for the comparison are new and were not available during the fitting of UNIFD group parameters, thus only the predictive abilities of the models were evaluated but not the correlative.

Some of the considered binary systems have a total pressure above atmospheric and the non-ideality of the vapor phase can influence the system behavior. Consequently, the accuracy of the VLE description was related not only to the accuracy of the activity coefficient model, but also to the accuracy of the vapor phase model. Therefore, the predictive models were compared by applying the same EOS for the description of the vapor phase non-ideality. SRK EOS [5] was

chosen in publications II - XIII for the vapor phase description, because the UNIFAC and UNIFD model parameters were optimized using SRK EOS.

In this work, COSMO-RS (COSMOtherm, 2012 version) and UNIFD are compared, though the 2005 version of the COSMOtherm program was used in papers VIII - XIII. In the newer version of the COSMOtherm program, the improvement of the conformer treatment (2008 release, [58]) and refinement of the parameters associated with sulfur and phosphorous as elements (2010 release, [30]) were introduced; namely the hard sphere radii specific to the elements and the parameter of vdW interactions were improved in the newer version.

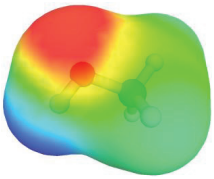
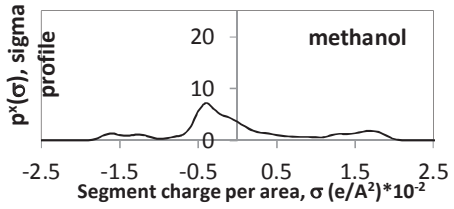
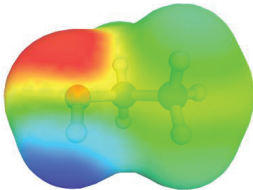
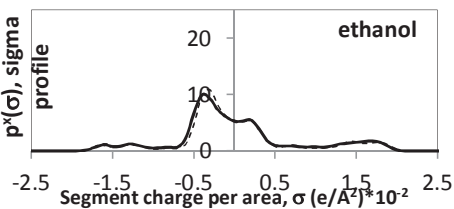
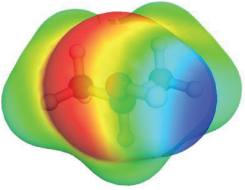
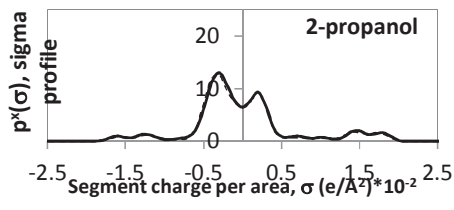
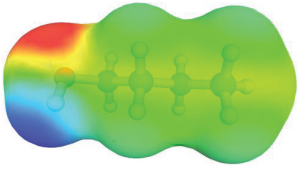
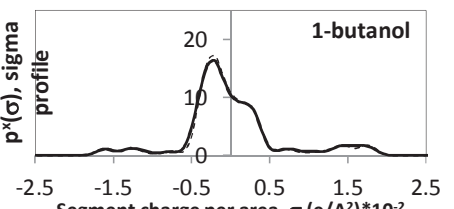
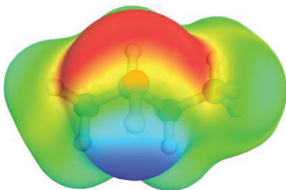
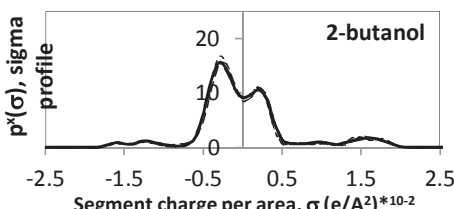


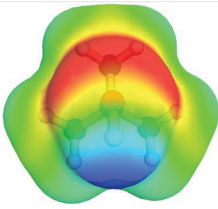
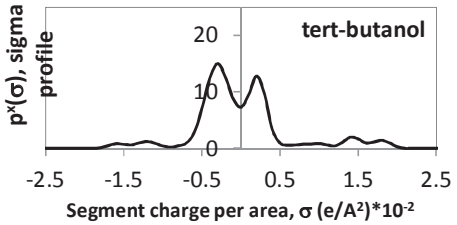
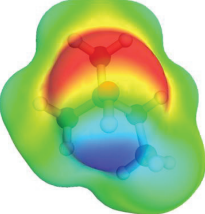
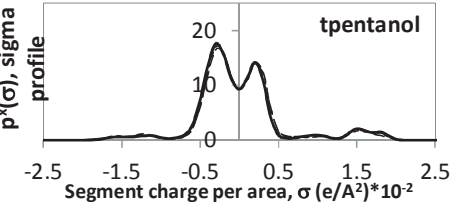
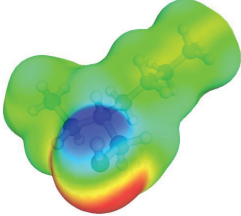
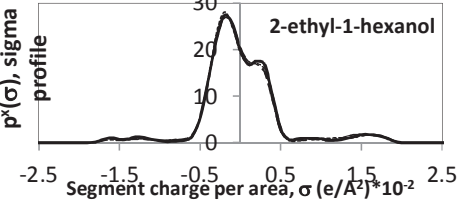
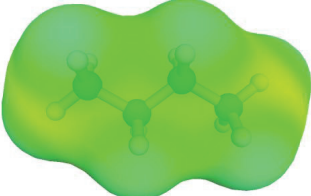
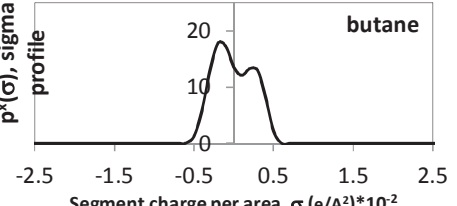
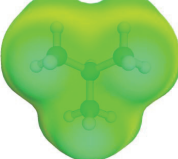
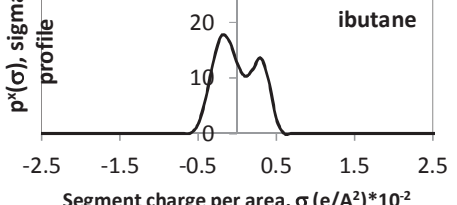
### 3.4.1 Details of the COSMO-RS calculations

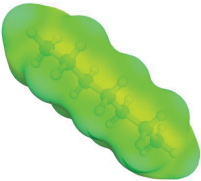
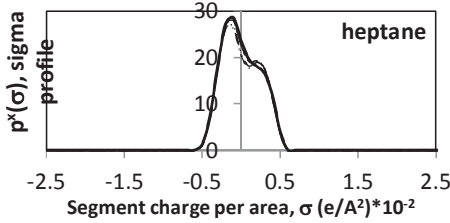
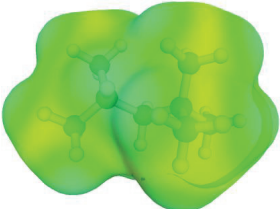
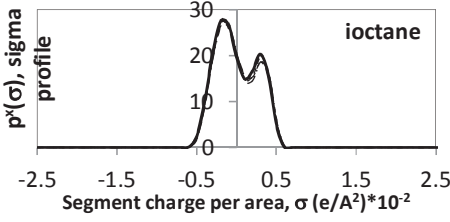
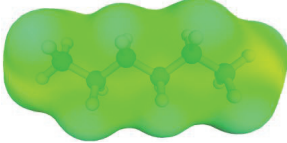
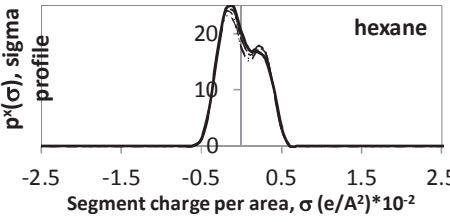
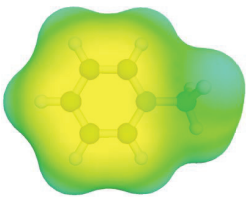
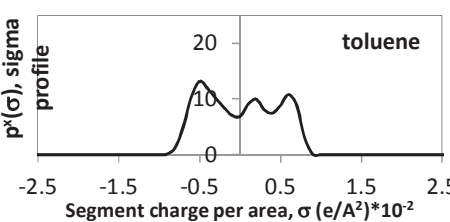
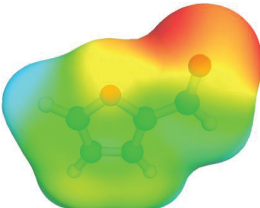
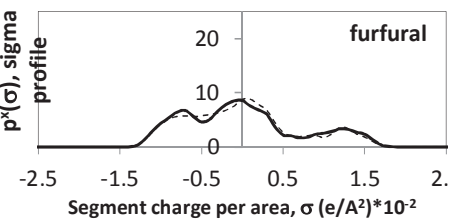
The procedure for COSMO-RS calculations had several steps. First, a conformer search has been made for the molecules under interest. HyperChem software [59] and the PM3 semiempirical computational method [60] was used for this purpose. Several conformers with the lowest energies were included in the calculations (Table 3.4.1). Then density functional theory (DFT) calculations were performed using the resolution of identity (RI) approximation with a TZVP basis set and BP functional as implemented in the Turbomole program (version 5.8 – 5.9). This combination of quantum methods and approximations has been recommended by the COSMOtherm authors and the parameters of the COSMOtherm have been optimized concerning the structures generated using this method combination [26]. It has also been shown [61] that a variation of the calculation techniques or the QM software can change the results of thermodynamic calculations. The resulting QM file that describes the screening surface charge density of the molecule in the ideal conductor was used in COSMOtherm program (versions 2012).

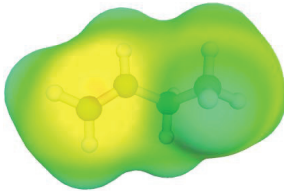
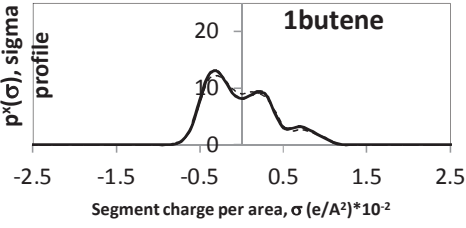
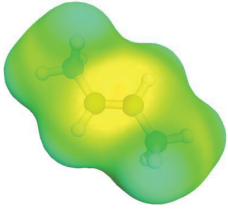
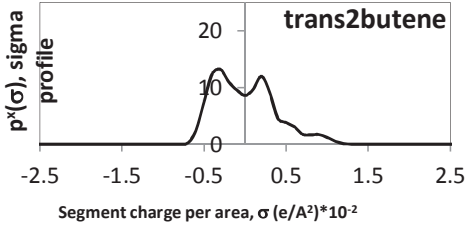
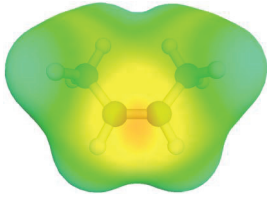
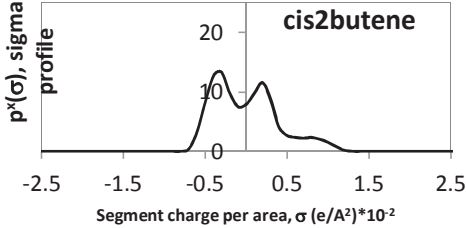
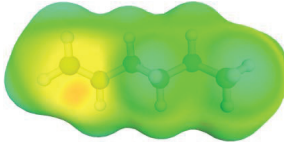
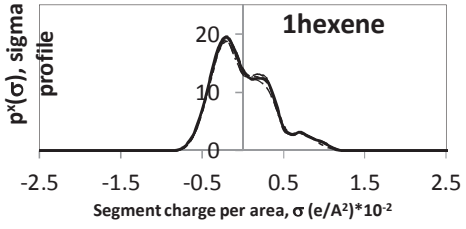
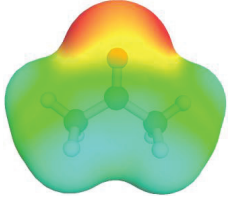
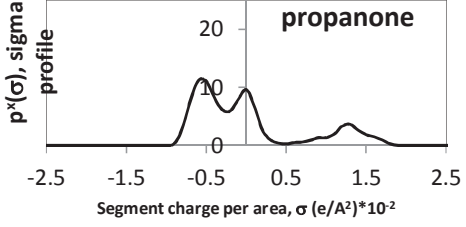
In Table 3.4.1 a list of compounds is provided with the number of conformers used. Additionally, the sigma profiles (histogram of the screening surface charge density) of the molecules are given in the table for the compounds under consideration. The sigma profile (see chapter 2.5.2) is a two-dimensional characteristic of the molecule surface charge density that is used in the COSMO-RS model as the basis for all calculations. Table 3.4.1 shows the sigma profiles of the five lowest-in-energy conformers of the compounds. In the COSMO-RS model (as implemented in the COSMOtherm software), the weighted sum of the sigma profiles is used for the treatment of molecule conformers.

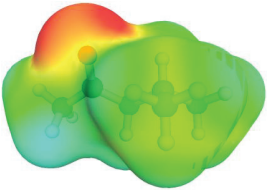
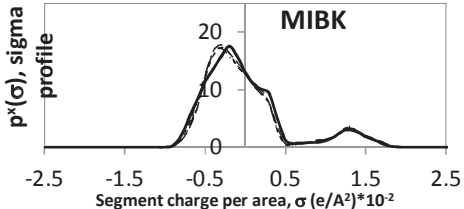
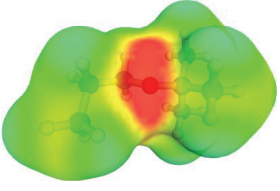
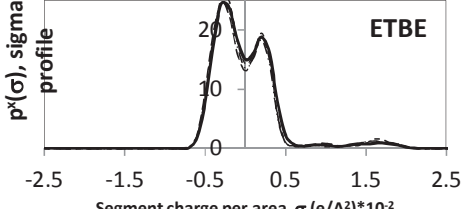
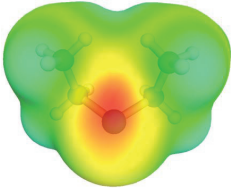
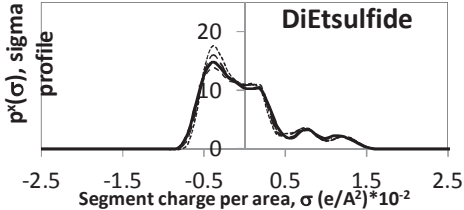
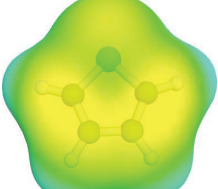
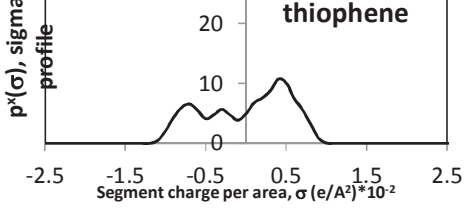
Table 3.4.1. List of compounds with number of conformers used in the calculations, screening surface charge density distribution of the molecules and the molecule sigma profiles.

Comp. / # conf.	Sigma surface of lowest conf.	Sigma profiles
Methanol 1		
Ethanol 2		
2-propanol 2		
1-butanol 2		
2-butanol 4		

Comp. / # conf.	Sigma surface of lowest conf.	Sigma profiles
Tert-butanol 1		
Tert-pentanol 3		
2-ethyl-1-hexanol 5		
Butane 1		
Iso-butane 1		

Comp. / # conf.	Sigma surface of lowest conf.	Sigma profiles
Heptane 9		
Iso-octane 4		
Hexane 9		
Toluene 1		
Furfural 2		

Comp. / # conf.	Sigma surface of lowest conf.	Sigma profiles
1-butene 3		 <p><b>1butene</b></p>
Trans-2-butene 1		 <p><b>trans2butene</b></p>
Cis-2-butene 1		 <p><b>cis2butene</b></p>
1-hexene 9		 <p><b>1hexene</b></p>
2-propanone 1		 <p><b>propanone</b></p>

Comp. / # conf.	Sigma surface of lowest conf.	Sigma profiles
MIBK 4		 <p style="text-align: center;"><b>MIBK</b></p>
ETBE 4		 <p style="text-align: center;"><b>ETBE</b></p>
DiEtsulfide 5		 <p style="text-align: center;"><b>DiEtsulfide</b></p>
Thiophene 1		 <p style="text-align: center;"><b>thiophene</b></p>

### 3.4.2 Alcohols

There are five articles presented in this thesis covering the phase behavior for a range of alcohols: methanol, ethanol, 2-propanol, 1-butanol, 2-butanol, tert-butanol, tert-pentanol, 2-ethyl-1-hexanol (II, III, IV, V, VII). A comparison of the predictive models shows that the UNIFD model is much more accurate than COSMO-RS in predicting the VLE measurement of binary systems containing alcohols and trans-2-butene, n-butane or i-butane (Figures 3.4.1 and 3.4.2 (a) and (b)). Only in tert-butanol-containing binaries, the two models are comparable (see Figures 3.4.1 and 3.4.2 (c)).

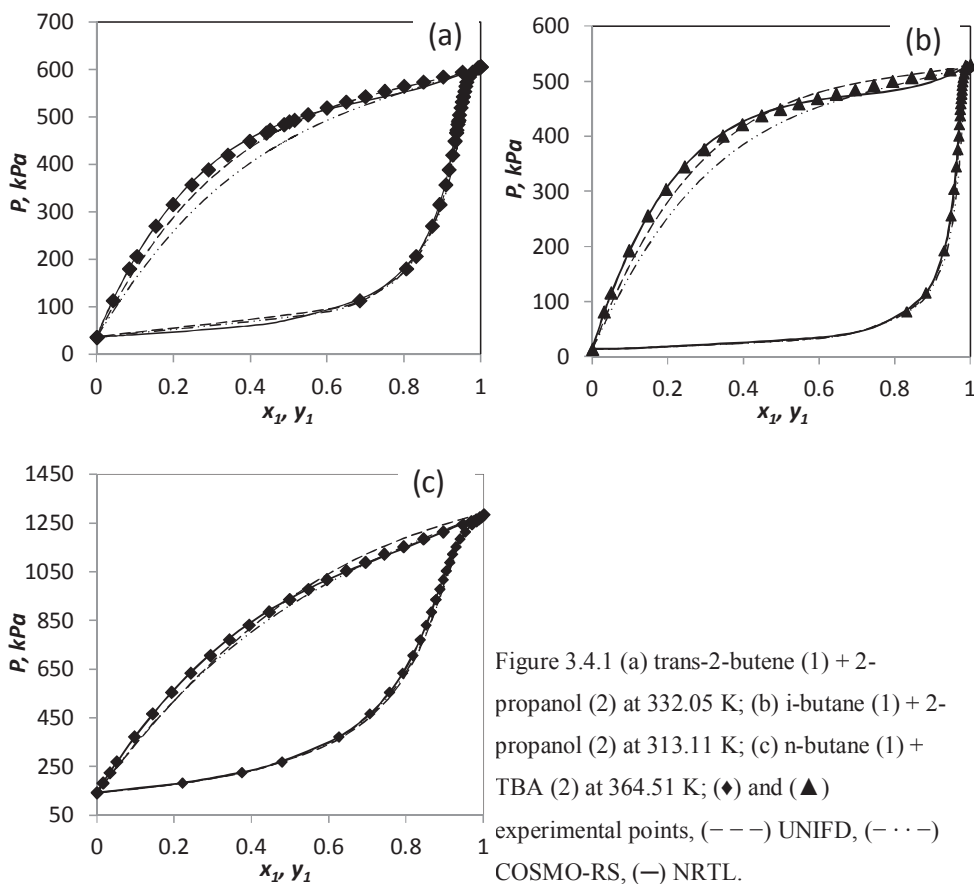


Figure 3.4.1 (a) trans-2-butene (1) + 2-propanol (2) at 332.05 K; (b) i-butane (1) + 2-propanol (2) at 313.11 K; (c) n-butane (1) + TBA (2) at 364.51 K; ( $\blacklozenge$ ) and ( $\blacktriangle$ ) experimental points, (---) UNIFD, (- · - ·) COSMO-RS, (—) NRTL.

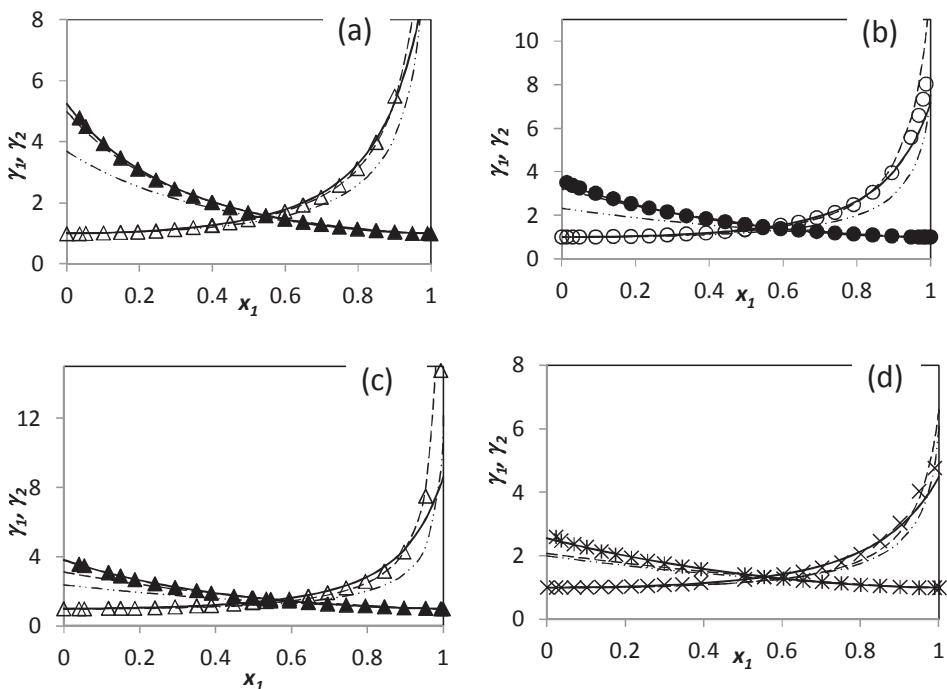


Figure 3.4.2. Activity coefficients in binary systems of (a) trans-2-butene(1) + ethanol (2) at 332.07K, (b) n-butane(1) + 1-butanol (2) at 364.5 K, (c) i-butane (1) + 2-butanol (2) at 313.08 K (d) trans-2-butene (1) + TBA (2) at 332.09K. (---) UNIFD, (- · - ·) COSMO-RS, (—) NRTL.

In a diluted solution of the alcohols in i-butane or n-butane, the description of COSMO-RS is comparable with UNIFD (Figures 3.4.3 and 3.4.4 (b)), whereas for the infinite dilution activity coefficients of alkanes in alcohol, the UNIFD predictions are closer to the experimental values when compared to COSMO-RS (Figures 3.4.3 and 3.4.4 (a)). Extensive comparison of the infinite dilution activity coefficients for alcohols in hydrocarbons presented by Xue et al. [62] has also showed that COSMO-based model COSMO-SAC and UNIFD were of similar accuracy.

On average, COSMO-RS slightly underestimates the infinite dilution activity coefficients both with alkanes in alcohols and alcohols in alkanes. This conclusion is totally in line with the results of Gmehling's group research for the COSMO-RS (Oldenburg) model [61].



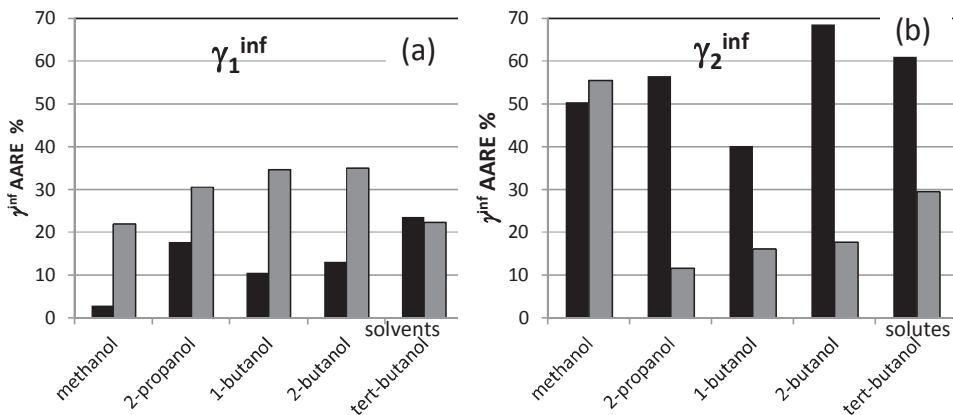


Figure 3.4.3. Average absolute relative error in infinite dilution activity coefficients of (a) n-butane in binary systems containing alcohols; (b) alcohols in binary systems containing n-butane at 364.5 K; black bar is UNIFD, gray bar is COSMO-RS.

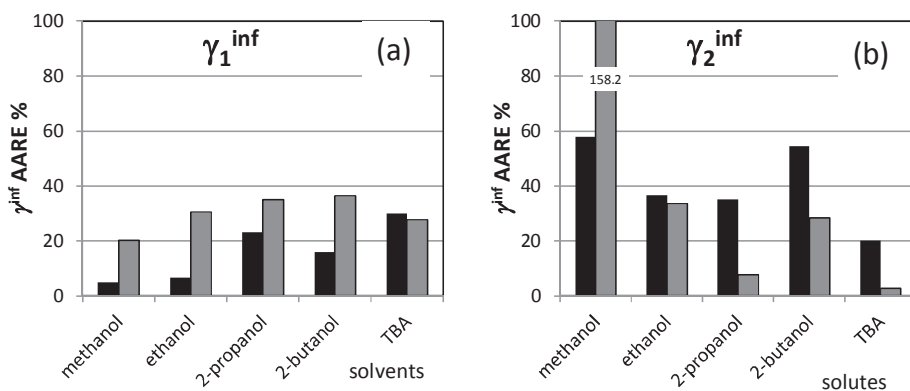


Figure 3.4.4. Average absolute relative error in infinite dilution activity coefficients of (a) i-butane in binary systems containing alcohols; (b) alcohols in binary systems containing i-butane at 313 K; black bar is UNIFD, gray bar is COSMO-RS.

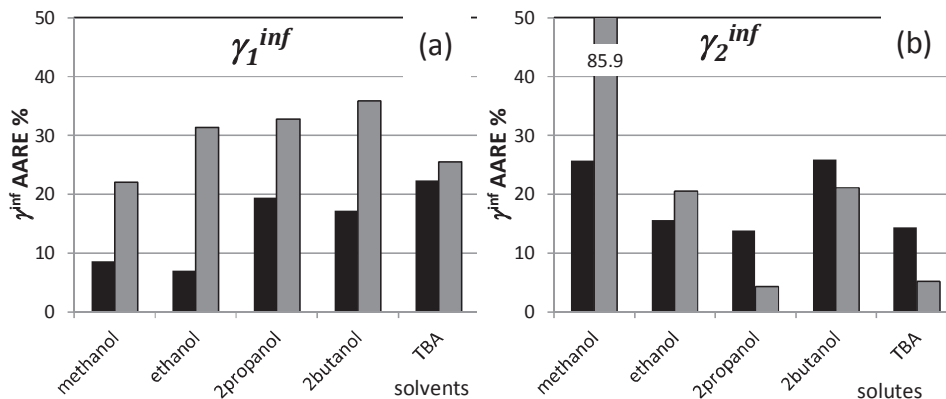


Figure 3.4.5. Average absolute relative error in infinite dilution activity coefficients of (a) trans-2-butene in binary systems containing alcohols; (b) alcohols in binary systems containing trans-2-butene at 364.5 K; black bar is UNIFD, gray bar is COSMO-RS.

In ketone (MIBK)- and aromatic (furfural)-containing systems, the infinite dilution activity coefficients of alcohols are also predicted more accurately with the COSMO-RS model (Figure 3.4.6).

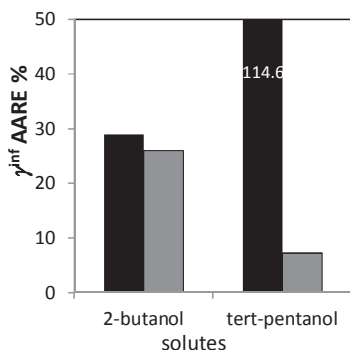


Figure 3.4.6. Average absolute relative error in percent for the infinite dilution activity coefficients of alcohols in MIBK or furfural at 368, 353 and 345 K; black bar is UNIFD, gray bar is COSMO-RS.

It is worth highlighting that the infinite dilution behavior of methanol is more accurately predicted with UNIFD than with the COSMO-RS model (Figures 3.4.3 - 3.4.5). This can be explained by

the separate group for methanol in the UNIFD model. However, activity coefficients in the moderate ranges of concentrations of methanol are predicted accurately with both UNIFD and COSMO-RS (Figure 3.4.7)

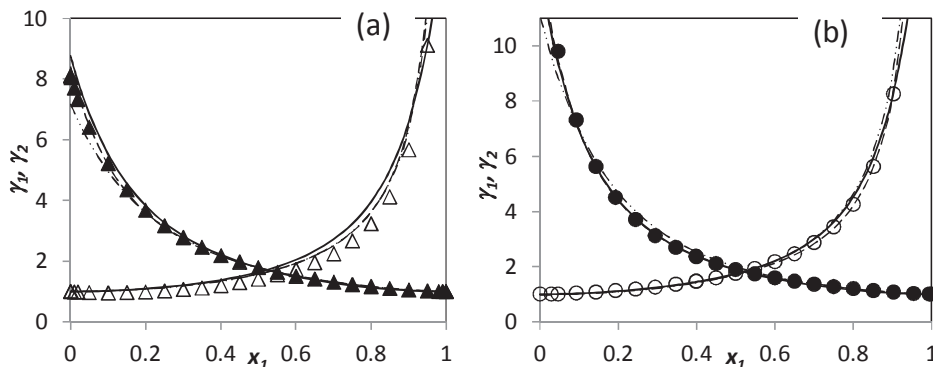


Figure 3.4.7. Activity coefficients in binary systems of (a) trans-2-butene (1) + methanol (2) at 332.07 K; (b) i-butane (1) + methanol (2) at 313.07 K; ( $\blacktriangle$ ) and ( $\bullet$ ) experimentally measured activity coefficients for the first component, ( $\Delta$ ) and ( $\circ$ ) experimentally measured activity coefficients for methanol, (---) UNIFD, (- · -) COSMO-RS, (-) NRTL.

To sum up, it can be concluded that the important properties of alcohol-containing systems are described less accurately in the COSMO-RS model in comparison with UNIFD and thus COSMO-RS is not recommended for alcohol-containing mixtures. Spuhl and Arlt [34] also concluded that the accuracy of COSMO-RS is not high when describing self-associating mixtures, such as alcohol and ethers. The better accuracy of the UNIFD model was also observed for alcohol-alkane systems in comparison with another COSMO-RS type model (i.e. COSMO-RS (Oldenburg) model from the Gmehling group [62, 63, 64]).

### 3.4.3 Ketones

Two articles are presented in this work covering VLE measurement and predictions for ketone-containing systems, i.e. 2-propanone- and MIBK-containing binaries (publications III and VI). The MIBK is a relatively small ketone represented by four functional groups in the UNIFD model. 2-propanone is the smallest molecule among the ketones and a comparison of the UNIFD and COSMO-RS models on 2-propanone-containing systems shows the ability of the two models to predict the behavior of the homological group outlier. The second components in the binary

systems are alkanes, alkenes, and alcohols. The results obtained for 2-propanone binary systems are shown in Figures 3.4.8 – 3.4.10.

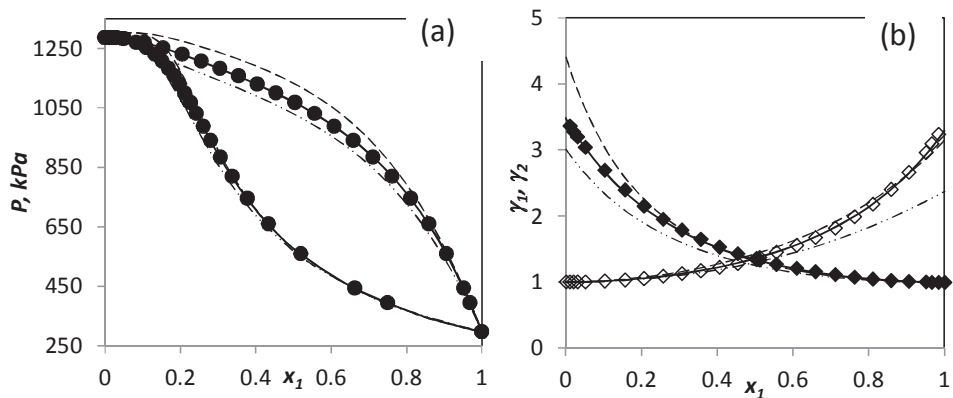


Figure 3.4.8. (a) pressure composition diagram for binary system 2-propanone (1) + n-butane (2) at 364.5 K (b) activity coefficients in 2-propanone (1) + i-butane (2) system at 364.5 K; (•), (◆) and (◇) are experimental points; (---) UNIFD, (- · - ·) COSMO-RS, (-) NRTL models.

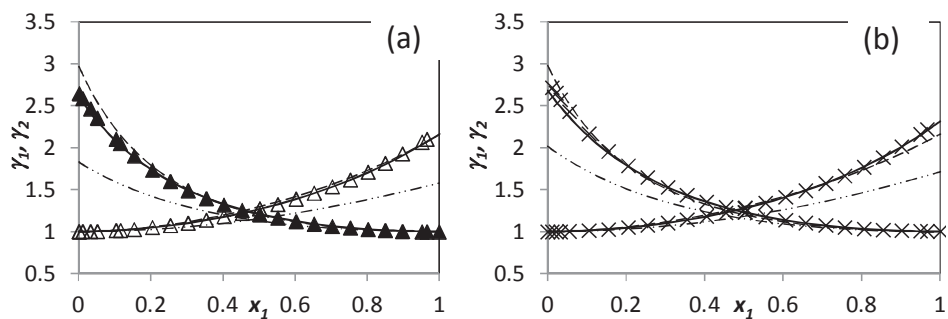


Figure 3.4.9. Activity coefficients in the binary systems of 2-propanone (1) and (a) + cis-2-butene at 365.5 K (2) (b) + trans-2-butene at 364.5 K; (▲), (Δ) and (×) are experimental points; (---) UNIFD, (- · - ·) COSMO-RS, (-) NRTL models.

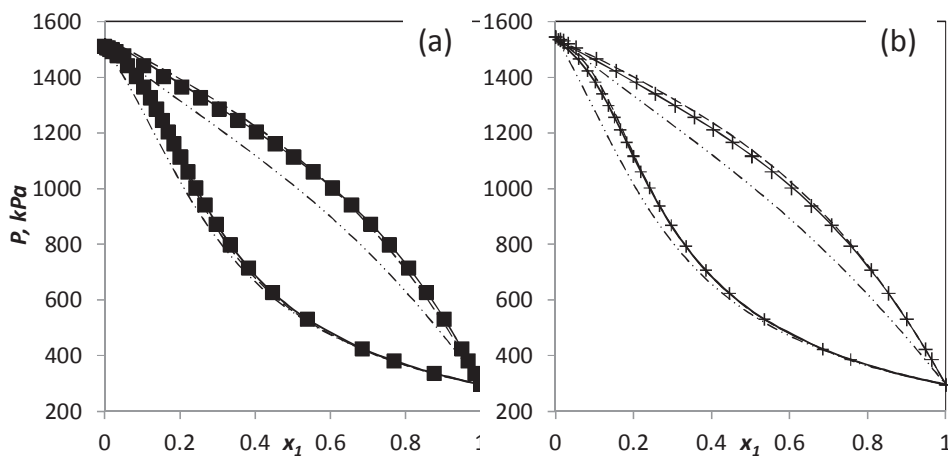


Figure 3.4.10. Pressure composition diagram for binary system 2-propanone (1) (a) + 1-butene (2), (■) experimental points; (b) + iso-butene at 364.5 K, (+) experimental points; (---) UNIFD, (- · · -) COSMO-RS, (-) NRTL models.

It can be seen that the UNIFD model predictions are much closer to the experimentally measured values in all systems except for 2-propanone + n-butane, where the predictions are comparable. This is an unexpected result because often the group contribution methods are not very accurate for the smallest molecules of the homological series (see publications I), whereas a priori methods (like the COSMO-RS) do not have such limitations.

In all the investigated binary systems containing alcohols (MIKB + 2-butanol, + tert-pentanol, + 2-ethyl-1-hexanol), COSMO-RS considerably underestimates the activity coefficients, whereas UNIFD slightly overestimates them (Figure 3.4.11).

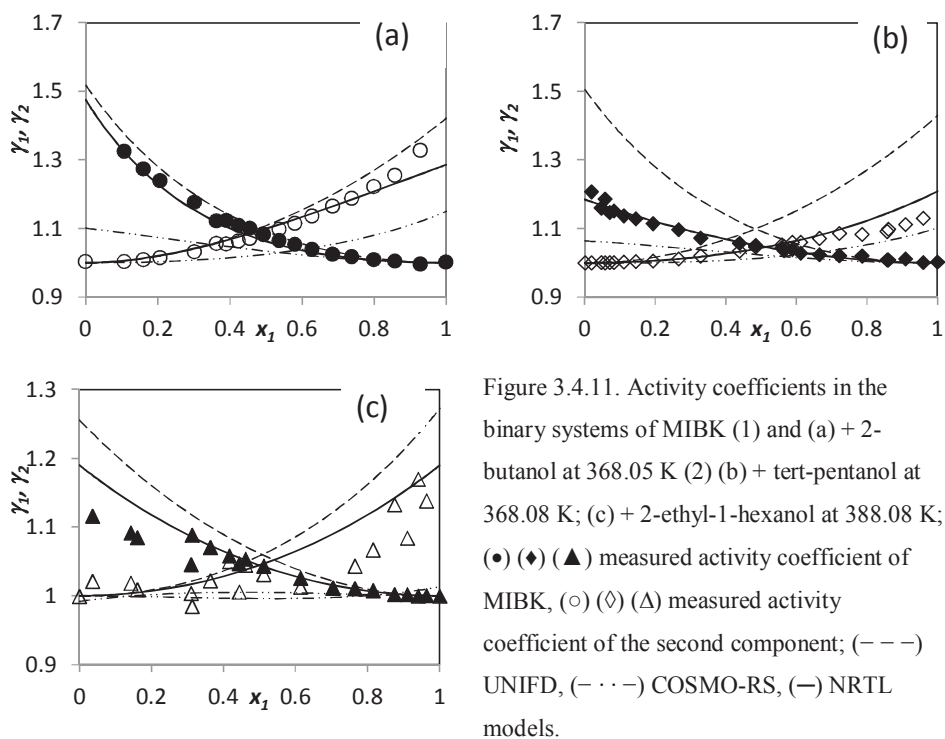


Figure 3.4.11. Activity coefficients in the binary systems of MIBK (1) and (a) + 2-butanol at 368.05 K (2) (b) + tert-pentanol at 368.08 K; (c) + 2-ethyl-1-hexanol at 388.08 K; (●) (◆) (▲) measured activity coefficient of MIBK, (○) (◇) (Δ) measured activity coefficient of the second component; (---) UNIFD, (- · - ·) COSMO-RS, (-) NRTL models.

The average error of the prediction of infinite dilution activity coefficients in the MIBK- and 2-propanone-containing systems is shown in Figures 3.4.12. In the investigated systems, COSMO-RS shows a slightly better prediction of the infinite dilution activity coefficients of ketones in alkanes and alkenes. The number of systems considered is, however, very limited for general conclusions. In the work of Xue et al. [64], the UNIFD model shows only a 15.6% deviation for 313 experimental infinite dilution activity coefficients for ketone. No value is given in the same paper for the deviation of COSMO-RS (Oldenburg) model predictions for ketones. Spuhl and Arlt [34] reported a deviation of up to 10% for COSMO-RS calculations of the activity coefficient in the infinite dilution range for alcohol-ketone systems, which is in line with our finding of an average 13% deviation for the investigated systems.

In comprehensive comparisons of the UNIFD and COSMO-RS (Oldenburg) models for VLE data [63], UNIFD was found to be more accurate both for alkane-ketone and alcohol-ketone systems.

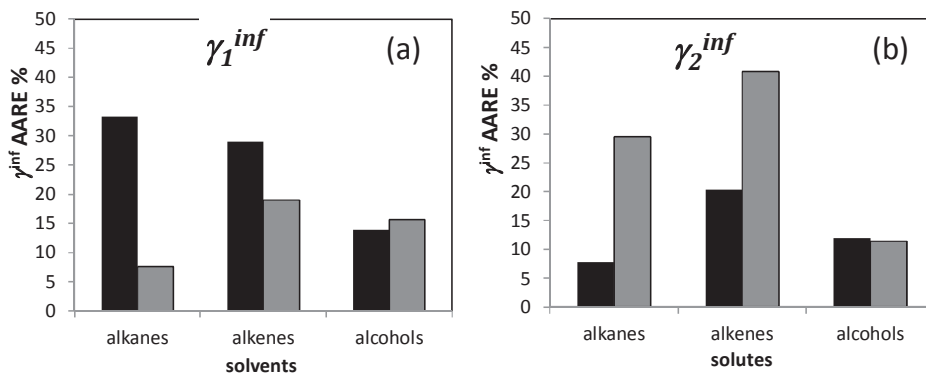


Figure 3.4.12. Average absolute relative error in infinite dilution activity coefficients of (a) MIBK and 2-propanone in binary systems containing alkanes, alkenes and alcohols; (b) alkanes, alkenes and alcohols in binary systems containing ketones (2-propanone and MIBK); black bar is UNIFD, gray bar is COSMO-RS.

### 3.4.4 Diethyl sulfide

Vapor-liquid equilibria were measured for seven binary systems containing diethyl sulfide in mixture with alkanes (heptane, hexane and isooctane), 1-hexene, cyclohexane, toluene and ETBE. The UNIFD group contributions of the  $\text{CH}_2\text{-S}$  sulfur group are not available for the public, thus only a comparison of the original UNIFAC method is possible. In the original UNIFAC, only the  $\text{CH}_2\text{-S}$  and  $\text{-CH}_2\text{-}$  group interaction parameter is available. Thus only diethyl sulfide + alkane and diethyl sulfide + cyclohexane systems can be predicted with the UNIFAC model (the cyclo carbon atom is represented by the same alkane  $\text{-CH}_2\text{-}$  group in the UNIFAC model).

As shown in Figure 3.4.13, the COSMO-RS predictions are usually better or comparable with the UNIFAC predictions. It is worth noting that the 2005 version of COSMO-RS has some difficulties in the description of these systems. The calculations were improved by removing the vdW interaction term (publication VIII). In later versions of the COSMOtherm software, the description of vdW interactions was improved (version 2010). The calculations presented here for the diethyl sulfide-containing systems include the improved description of vdW interactions and, thus, are more accurate.

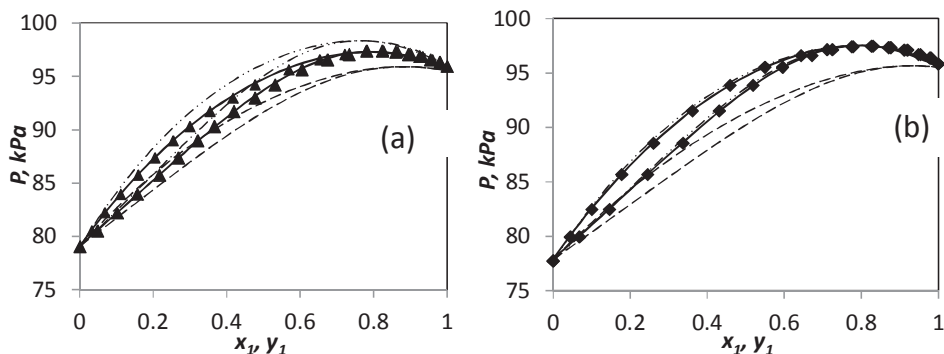


Figure 3.4.13. Pressure composition diagram for binary system diethyl sulfide (1) (a) + n-heptane (2); (b) + isooctane (2) at 363.15 K; (▲) and (◆) experimental points; (---) UNIFD, (- · - ·) COSMO-RS, (-) NRTL models.

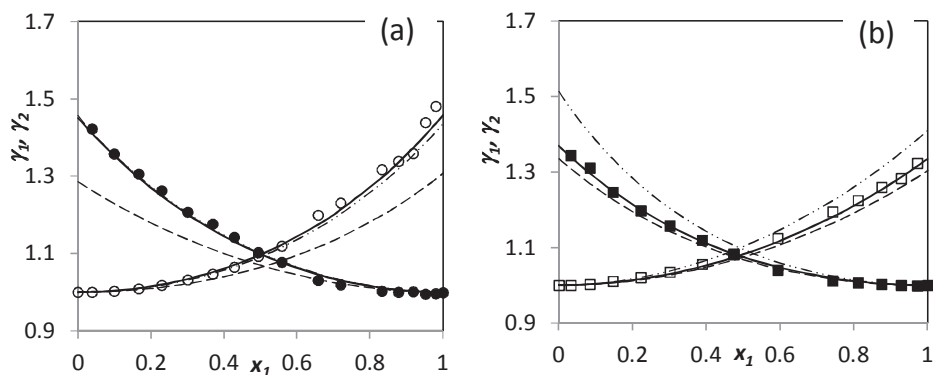


Figure 3.4.14. Activity coefficients in the binary systems of diethyl sulfide (1) and (a) + n-hexane at 338.15 K (2) (b) + cyclohexane at 343.15 K; (●) (■) measured activity coefficient of diethyl sulfide, (○) (□) measured activity coefficient of the second component; (---) UNIFAC, (- · - ·) COSMO-RS, (-) NRTL models.

As expected, in 1-hexene and ETBE mixtures with diethyl sulfide, the prediction of activity coefficients with COSMO-RS is closer to the experimental values compared to the UNIFAC model predictions due to the absence of corresponding parameters in the UNIFAC model (Figure 3.4.15).



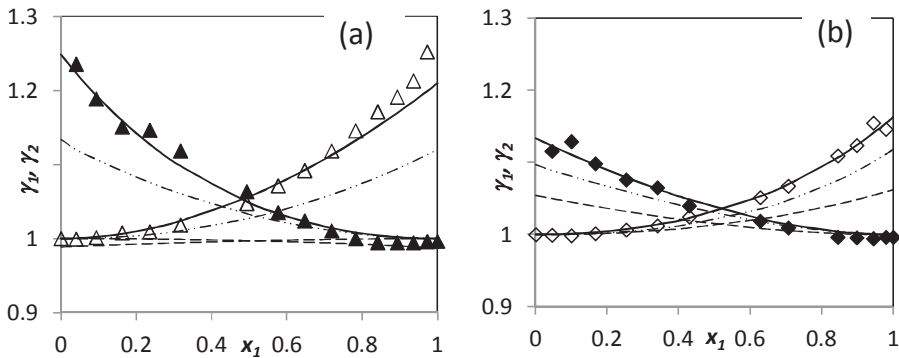


Figure 3.4.15. Activity coefficients in the binary systems of diethyl sulfide (1) and (a) + 1-hexene, (b) + ETBE (2) at 333.15 K; ( $\blacktriangle$ ) ( $\blacklozenge$ ) measured activity coefficient of diethyl sulfide, ( $\triangle$ ) ( $\diamond$ ) measured activity coefficient of the second component; (---) UNIFAC, (- · - ·) COSMO-RS, (—) NRTL models.

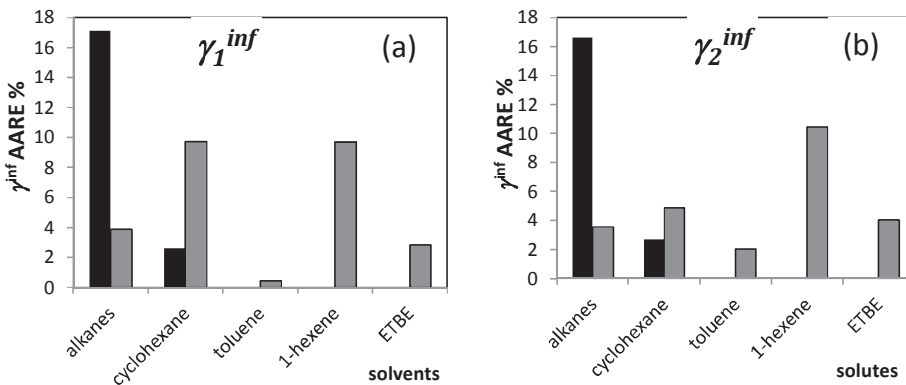


Figure 3.4.16. Average absolute relative error in infinite dilution activity coefficients of (a) diethyl sulfide in the binary systems with different solvents; (b) solutes in diethyl sulfide; black bar is UNIFAC, gray bar is COSMO-RS.

The activity coefficients of the investigated systems are close to one and the errors of the predictions are not large in absolute value. Infinite dilution activity coefficient errors are shown in Figure 3.4.16. The relative deviations of the UNIFAC model for the alkane + diethyl sulfide mixtures are moderate, whereas COSMO-RS shows errors lower than 10 % for all the investigated binaries containing diethyl sulfide.

The mixtures with sulfur-containing compounds were not included in the comparative review of the UNIFD and COSMO-RS (Oldenburg) models made by the Gmehling group [62,63]. To the

author's knowledge, there are no publications that have compared the relative accuracy of the UNIFD or UNIFAC models with the COSMO-RS model on mixtures containing sulfur compounds. However, the UNIFD and COSMO-RS models can be compared if the corresponding UNIFD parameters would be publicly available. In accordance with the UNIFD parameters table published in [22], the sulfur group parameters of diethyl sulfide with other groups have been optimized but have not been published.

### 3.4.5 Thiophene

Vapor-liquid equilibria for binary systems containing thiophene were published in manuscripts VIII, XII, XIII. The second components of the binary mixtures were alkanes (hexane and isooctane), toluene, and ETBE. The UNIFD model group contribution parameters for thiophene were published in [18] and in contrast to the original UNIFAC model, thiophene is not presented as a separate group in the UNIFD model.

The accuracy of both models in the alkane-containing systems is satisfactory, see Figure 3.4.17. In particular, UNIFD is better in the isooctane binary (Figure 3.4.17 (b)), whereas COSMO-RS is slightly better in the binary mixture of thiophene with hexane (Figure 3.4.17 (a)).

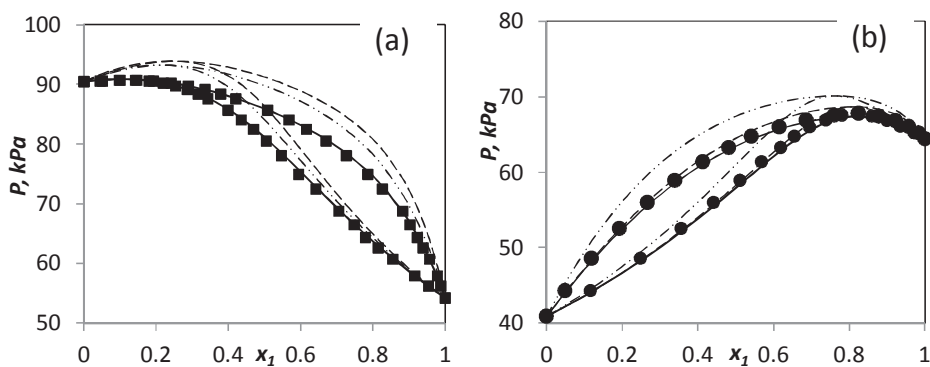


Figure 3.4.17. Pressure composition diagram for binary system of thiophene (1) (a) + n-hexane (2) at 338.15 K; (b) + isooctane (2) at 343.15 K; (■) and (●) experimental points; (---) UNIFD, (- · - ·) COSMO-RS, (-) NRTL models.

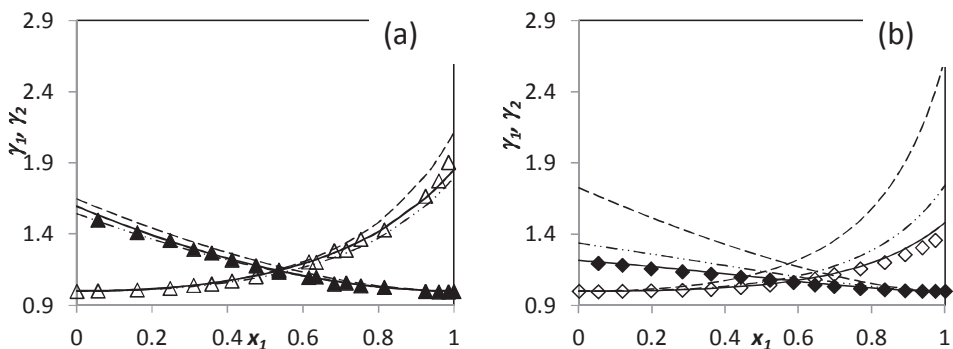


Figure 3.4.18. Activity coefficients in the binary systems of thiophene (1) and (a) + 1-hexene, (b) + ETBE (2) at 333.15 K; ( $\blacktriangle$ ) ( $\blacklozenge$ ) measured activity coefficient of diethyl sulfide, ( $\triangle$ ) ( $\diamond$ ) measured activity coefficient of the second component; (---) UNIFAC, (- · - ·) COSMO-RS, (—) NRTL models.

The activity coefficient of the 1-hexene- and ETBE-containing mixtures with thiophene are more accurately predicted with COSMO-RS, see Figure 3.4.18, because the ether group – aromatic sulfur group interaction parameter is not available in the published UNIFAC parameters. In the infinite dilution range, the activity coefficients are better estimated with the COSMO-RS model for toluene, 1-hexene, and ETBE binary mixtures with thiophene, see Figure 3.4.19, with the exception of thiophene infinite dilution activity coefficients in hexane and isooctane.

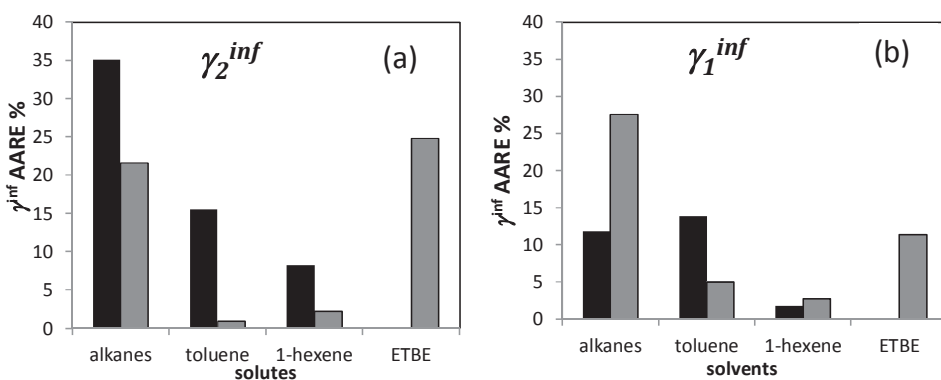


Figure 3.4.19. Average absolute relative error in infinite dilution activity coefficients of (a) thiophene in binary systems with different solvents; (b) solutes in thiophene; black bar is UNIFAC, gray bar is COSMO-RS.

Though the number of binary systems considered is small, we can conclude that the current version of COSMO-RS is better for predicting the behavior of thiophene-containing systems than the UNIFD model. At the same time, as shown in publications XII and XIII, the original UNIFAC model is more accurate in predictions of thiophene + alkanes system activity coefficients in comparison with COSMO-RS.

### 3.4.6 Furfural

A large set of experimental data for furfural-containing binary systems was published in paper II. The results are presented in Figures 3.4.20 – 3.4.25. Furfural is treated in the UNIFAC and UNIFD models as a separate group and thus a better accuracy is expected with the UNIFD model in comparison with the COSMO-RS model.

Both models predict the behavior of the furfural + MIBK binary system well (Figures 3.4.20 – 21), although the infinite dilution activity coefficients of MIBK are overestimated by both models.

The accuracy of the vapor-liquid equilibria predictions for furfural + alcohol systems with UNIFD and COSMO-RS varies at different temperatures (Figures 3.4.22 – 24). On average the COSMO-RS predictions are slightly closer to the experimental values than the UNIFD predictions.

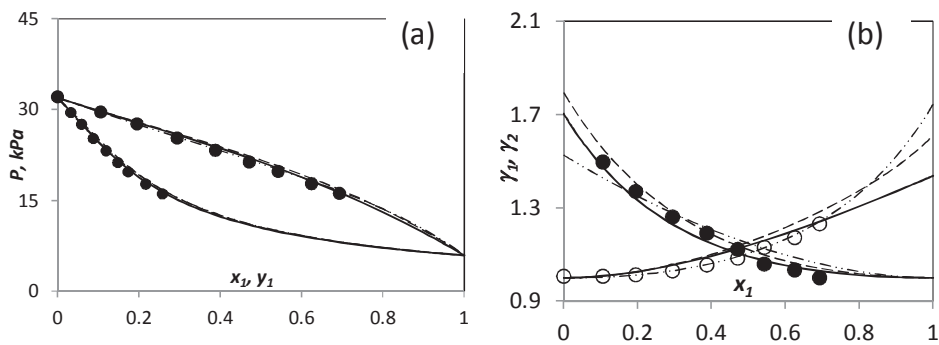


Figure 3.4.20. Binary system of furfural (1) + MIBK (2) at 353.3 K; (a) Pressure composition diagram; (b) activity coefficients; ( $\bullet$ ), ( $\circ$ ) experimental points, (---) UNIFAC, (- · - ·) COSMO-RS, (—) NRTL models

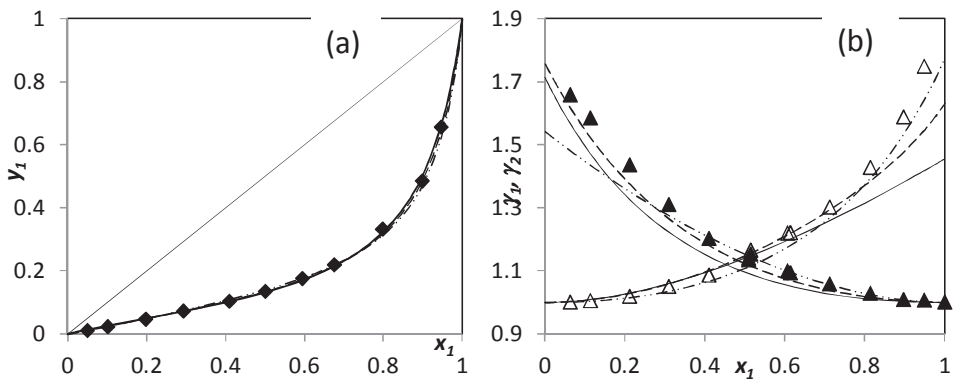


Figure 3.4.21. Binary system of furfural (1) + MIBK (2); (a) liquid composition – vapor composition diagram at 333.3 K; (b) activity coefficients at 345.8 K; (▲), (Δ) experimental points, (---) UNIFAC, (- · - ·) COSMO-RS, (-) NRTL models

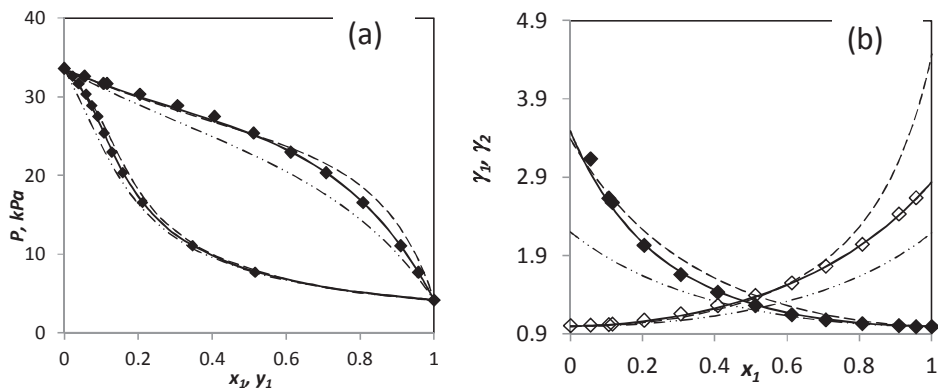


Figure 3.4.22. (a) pressure composition diagram for binary system furfural (1) + 2-butanol (2) at 345.7 K (b) activity coefficients in furfural (1) + 2-butanol (2) system at 345.7 K; (◆) and (◇) are experimental points; (---) UNIFD, (- · - ·) COSMO-RS, (-) NRTL models.

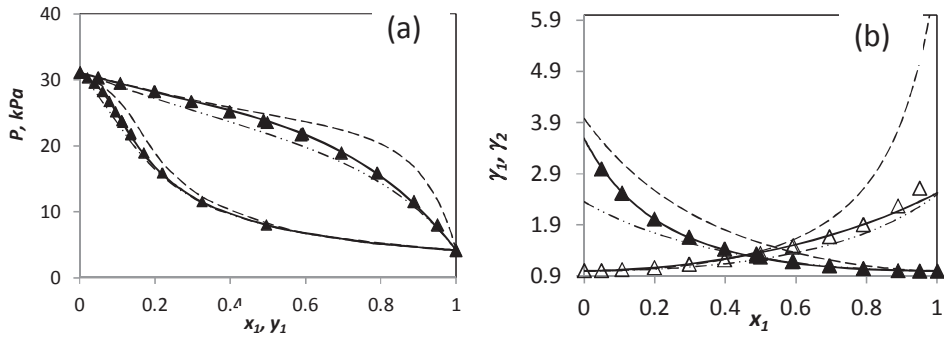


Figure 3.4.23. (a) pressure composition diagram for binary system furfural (1) + tert-pentanol (2) at 345.6 K (b) activity coefficients in furfural (1) + tert-pentanol (2) system at 345.6 K; ( $\blacktriangle$ ) and ( $\triangle$ ) are experimental points; (---) UNIFD, (- · - ·) COSMO-RS, (—) NRTL models.

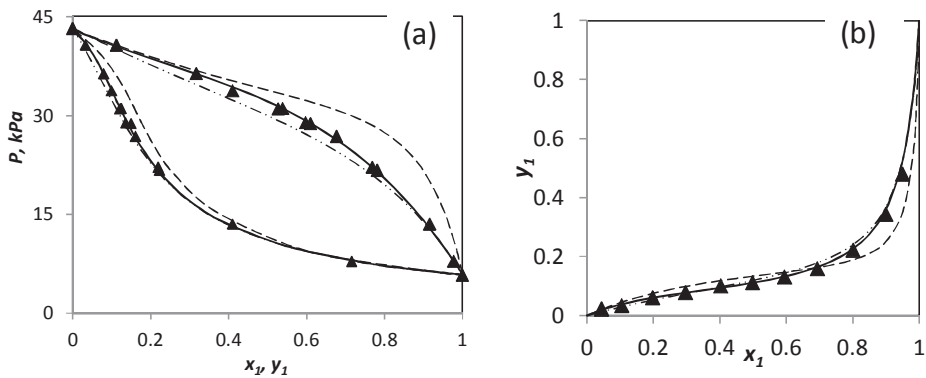


Figure 3.4.24. Binary system furfural (1) + tert-pentanol (2); (a) pressure composition diagram for at 353.2 K; (b) liquid composition – vapor composition diagram at 333.3 K; ( $\blacktriangle$ ) are experimental points; (---) UNIFD, (- · - ·) COSMO-RS, (—) NRTL models.

At infinite dilution conditions, on average UNIFD predicts furfural activity coefficients more accurately, whereas the COSMO - RS model is better on average for predictions of the infinite dilution activity coefficient for alcohols (Figure 3.4.25).

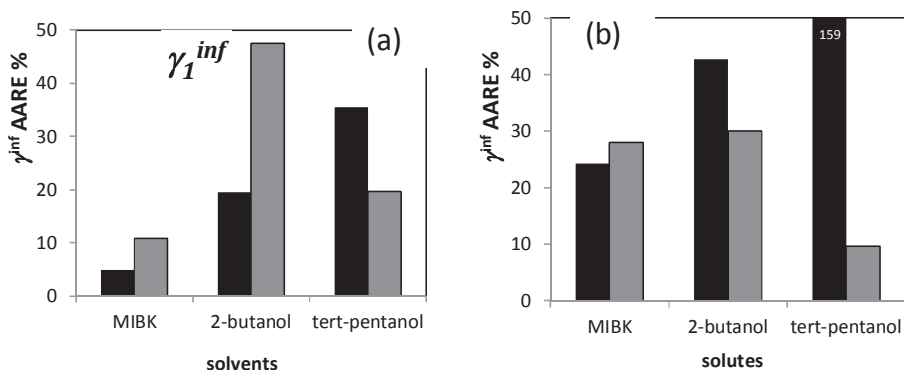


Figure 3.4.25. Average absolute relative error in infinite dilution activity coefficients of (a) furfural in binary systems with different solvents; (b) solutes in furfural; black bar is UNIFAC, gray bar is COSMO-RS.

To summarize, a review of the different types of COSMO-RS models was available in the literature [61,34]. The COSMO-RS version by Klamt [26,28] seems to be a more advanced model in comparison with COSMO-RS (Oldenburg), as it includes not only electrostatic and hydrogen bond interactions, but also dispersive interactions.

In order to focus on the predictive ability of the models rather than the correlative, only new experimental data were used for the comparison of COSMO-RS and UNIFD. Hence a smaller amount of experimental data was used than in other similar research studies [61, 34].

The presented comparison showed that UNIFD is on average considerably better for predicting the VLE in binary systems. However, if the UNIFD parameters are not available, the a priori predictive model COSMO-RS is a good alternative, as the prediction of the thermodynamic behavior of a compound can be made without the availability of any information apart from the chemical formula. COSMO-RS is a new model under extensive development. This means that any weaknesses of the model that are revealed (i.e. treatment of hydrogen bond forces and dispersive forces) can be improved in future.

### 3.5 Prediction of excess enthalpies with the UNIFAC-Dortmund and COSMO-RS models

The excess molar enthalpy ( $h^E$ ) of thirteen binary systems from publications II - XI was described with the UNIFD and COSMO-RS models. The experimental  $h^E$  data for the systems under consideration were obtained either in this work [II, III] or were found in the literature (see Table 3.5.1).

The accuracy of COSMO-RS predictions for alkane – alcohol systems is modest due to the imperfect description of associating mixtures by the COSMO-RS model, as mentioned in chapter 3.5.3.

Table 3.5.1. Summary of  $h^E$  data: measured and published in II - XI, available in the literature and calculated using the UNIFD and COSMO-RS models.

Comp. 1	Comp. 2	T, K; P, MPa	Number of points	Ref	$ \Delta h^E $ , J·mol <sup>-1</sup>	
					UNIFD	COSMO-RS, v.2012
n-butane	Methanol	298.15	23	[65]	37.7	488.3
		298.15	26	[66]	40.9	495.3
		323.15	26		24.4	568.5
		348.15	25		42.2	477.5
	1-butanol	298.15	33	[65]	23.5	360.5
		298.15 (5 MPa)	31	[67]	22.2	328.3
		323.15 (5 MPa)	28		32.6	254.8
		348.15 (5 MPa)	28		72.7	155.6
i-butane	2-propanol	298.15 (5 MPa)	30	[68]	100.9	250.0



Comp. 1	Comp. 2	T, K; P, MPa	Number of points	Ref	$ \Delta h^E $ , J·mol <sup>-1</sup>	
					UNIFD	COSMO-RS, v.2012
					323.15 (5 MPa)	18
Propanone	n-butane	263.15	9	[69]	96.5	846.9
MIBK	2-butanol	297.8	10	III	330.9	1021.0
		298.15	24	[70]	147.6	780.4
MIBK	Tert-pentanol	297.8	10	III	47.6	742.6
MIBK	Tert-pentanol	298.15	N/a	[71]	173.5	271.7
MIBK	2-ethyl-1-hexanol	297.8	10	III	76.3	975.8
Furfural	2-butanol	298.15	9	II	362.4	534
		308.15	10	[72]	79.1	73.0
	Tert-pentanol	298.15	9	II	109.7	316.24
	MIBK	298.15	9	II	820.5	84.0
Diethyl sulfide	Hexane	298.15	19	[73]	245.2	78.5
		298.15	19	[74]	242.7	76.0
	Heptane	303.15	11	[75]	295.6	85.2
	Cyclohexane	298.15	11	[76]	233.1	91.6

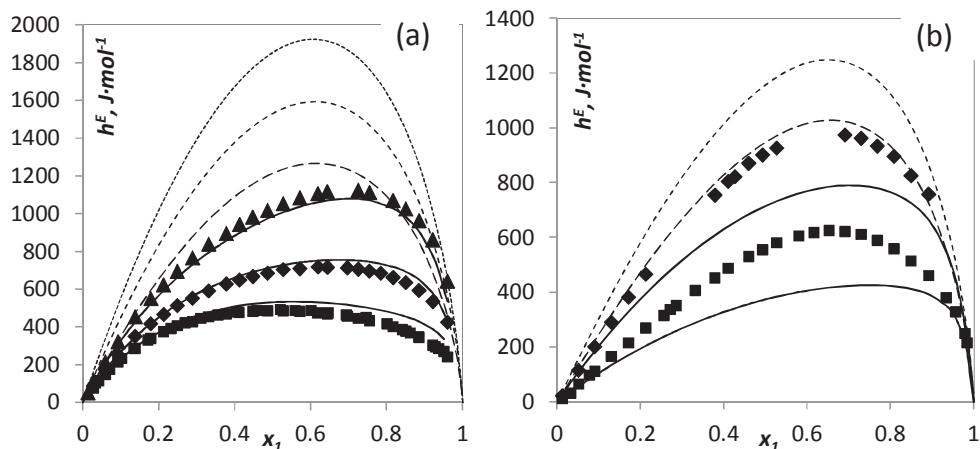


Figure 3.5.1. Molar excess enthalpy (a) in the butane + methanol system; (■), (◆) and (▲) are the experimental points from [68,69] at 298.15, 323.15 and 348.15 K respectively; (b) in the i-butane + 2-propanol system, (■) and (◆) are experimental points at 298.15 and 323.15 K respectively from [77]; (—) UNIFD model; (— —) COSMO-RS at 298.15 K, (- -) COSMO-RS at 323.15 K and (- · -) COSMO-RS at 348.15 K.

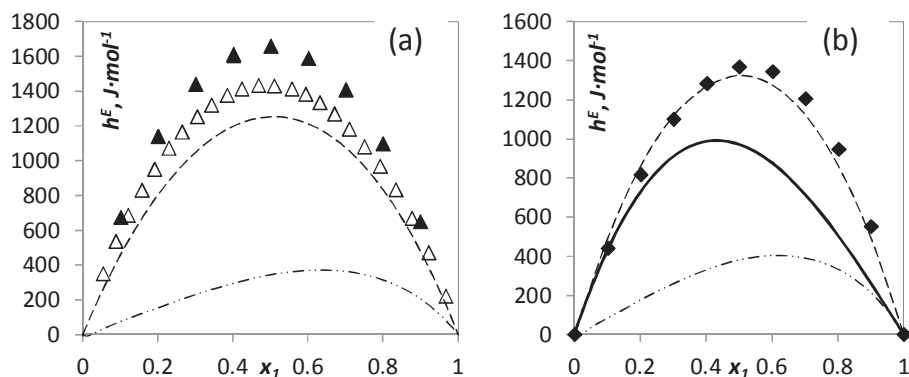


Figure 3.5.2. Molar excess enthalpy in the binary system of (a) MIBK (1) + 2-butanol (▲) experimental data at 297.8 K from publication III, (Δ) at 298.15 from [70]; (b) the MIBK(1) + tert-pentanol (2) system; (◆) experimental data at 297.8 K from publication III, (—) correlation of experimental data from [71] at 298.15; (— —) UNIFD, (- · · -) COSMO-RS at 297.8 K.

The UNIFD model shows a deviation from 7 to 22% of predicted molar excess enthalpy in the alkane + alcohol mixtures (the highest value is for the i-butane + 2-propanol mixture), whereas

COSMO-RS shows a deviation from 46 to 96% (Figure 3.5.1). Thus, COSMO-RS gives more than three times the relative deviation in comparison with the UNIFD model for ketone-containing systems (propanone + n-butane and MIBK + alcohols). However, the accuracy of the UNIFD model is not very high either, see Figure 3.5.2.

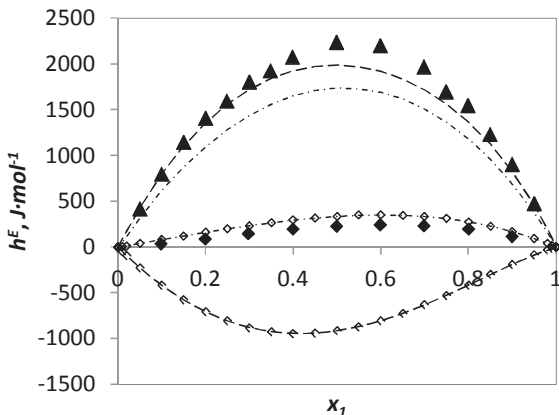


Figure 3.5.3. Excess molar enthalpy  $h^E$  at 298.15 K for furfural (1) + (2) tert-pentanol: (▲) measured  $h^E$  from publication II; (---) UNIFD; (-.-) COSMO-RS; furfural (1) + MIBK (2) (◆) measured from publication II; (-◇-) UNIFD; (-◇-.-) COSMO-RS.

In furfural-containing systems, the COSMO-RS prediction accuracy varies. The UNIFD model predicts the molar excess enthalpy of furfural + MIBK binary system incorrectly, but in the case of furfural + alcohol systems, the UNIFD predictions are much closer to the experimental values compared to COSMO-RS (Table 3.5.1, Figure 3.5.3).

In the systems containing diethyl sulfide, the UNIFD model was not applicable because of the absence of UNIFD parameters for the sulfide group, and consequently the predictions of the UNIFAC model were used for the comparison. Naturally, as the excess enthalpy data were not included in the fitting of the UNIFAC model parameters, the predictions of excess enthalpy with the UNIFAC model is poor (more than 60% deviation, Figure 3.5.4). The COSMO-RS model shows on average 19% deviation between the measured and predicted molar excess enthalpies in the diethyl sulfide binary systems under investigation.

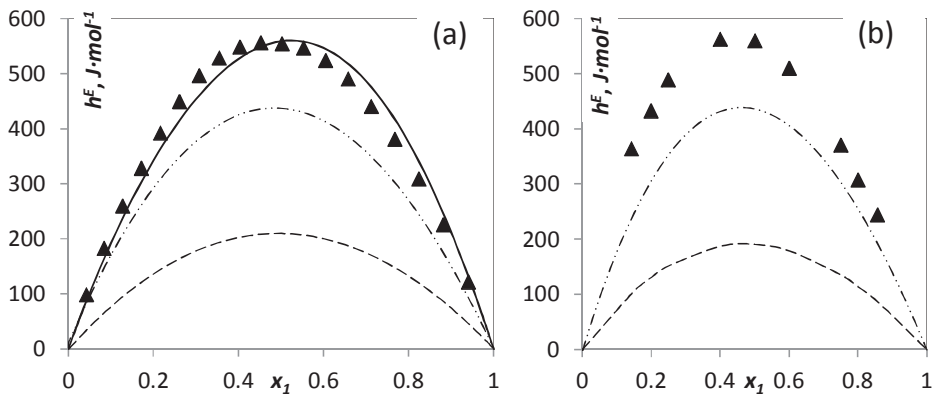


Figure 3.5.4. Molar excess enthalpy for (a) diethyl sulfide (1) + hexane (2) at 298.15 K; ( $\blacklozenge$ ) experimental points from [73], (—) correlation from [78]; (b) diethyl sulfide (1) + cyclohexane (2) ( $\blacktriangle$ ) experimental points at 298.15 K from [76]; (---) UNIFAC, (- · - ·) COSMO-RS.

To sum up, the UNIFD model is superior to COSMO-RS in terms of estimating the molar excess enthalpy of mixing in binary systems where UNIFD group parameters are available. The accuracy of COSMO-RS in  $h^E$  predictions can vary, but usually the deviation from the experimental value is more than 18%. These conclusions are in good agreement with the results of the comprehensive review of the COSMO-RS (Oldenburg) and UNIFAC methods made by Constantinescu et al. [64] on a large database of excess enthalpy data (Dortmund Data Bank).

### 3.6 Improvement of group contribution methods by distance weighting

As was shown in the previous chapters, commonly used predictive methods estimate the VLE and  $h^E$  behavior with an accuracy that cannot be predicted in advance. The same trend can be observed for the prediction of pure compound properties by group contribution methods (GCMs). However, in future a priori methods (like COSMO-RS) or other methods based on quantum calculations could become more accurate than GCMs; in the current situation, improvements in the existing group contribution methods seem to be more realistic. A new calculation procedure for GCMs was suggested in publications I. This procedure can improve the predictions of GCMs by utilizing the available computing power and the existence of the extended properties databases [79,80]. The main idea of the improvement is that the group contribution parameters can be derived for each prediction task separately, taking into account the similarity of the compound of the prediction and the database compounds.

When the similarity is taken into account using a comparison of the compound functional groups, the distance factor is defined as

$$d_j = \sum_{i=1}^{N_G} (n_{i,j} - n_{i,est})^2 + \left( \sum_{i=1}^{N_G} n_{i,j} - \sum_{i=1}^{N_G} n_{i,est} \right)^2 \quad (3.6.1)$$

where  $n_{i,j}$  is the number of group  $i$  in compound  $j$ ,  $n_{i,est}$  is the number of group  $i$  in a compound whose property is estimated, and  $N_G$  is the total number of groups in the GCM. The smaller the distance factor, the more similar the compounds are in respect of functional groups.

The thermodynamic property of component  $j$  ( $M_j$ ) is a function of the numbers of functional groups ( $n_{i,j}$ ) and the corresponding parameters  $a_i$  (group contributions):

$$M_j = a_0 + \sum_{i=1}^{N_G} a_i n_{i,j} \quad (3.6.2)$$

Thus, parameters  $a_i$  can be optimized using matrix inversion, taking into account the compound similarity through the distance weighting:

$$(a) = \left[ [n]^T [W] [n] \right]^{-1} [n]^T [W] (P_{meas}) \quad (3.6.3)$$

where  $W$  is the weight matrix with elements determined by the distance:

$$W_j = \frac{1}{d_j + \varepsilon} \quad (3.6.4)$$

Even though the idea of utilizing chemical similarity in group contribution methods seems to be intuitively obvious, it has not been mentioned or tested before in the open literature. In order to

test the idea, the GCMs of Joback – Reid [81] and of Marrero – Gani [82] were considered in publications I. An improvement in normal boiling point (NBP) predictions was proven for both GC methods using the suggested distance weighting procedure (DW). The database of normal boiling points was taken from the Engineering Handbook by Poling [83], where data for 386 hydrocarbons were collected. In Figure 3.6.1, the results of the prediction of NBP are presented for the original Joback and Reid GCM, for the proposed method where no weighting is used (diagonal elements of  $W$  matrix are equal to one), and for the DW method.

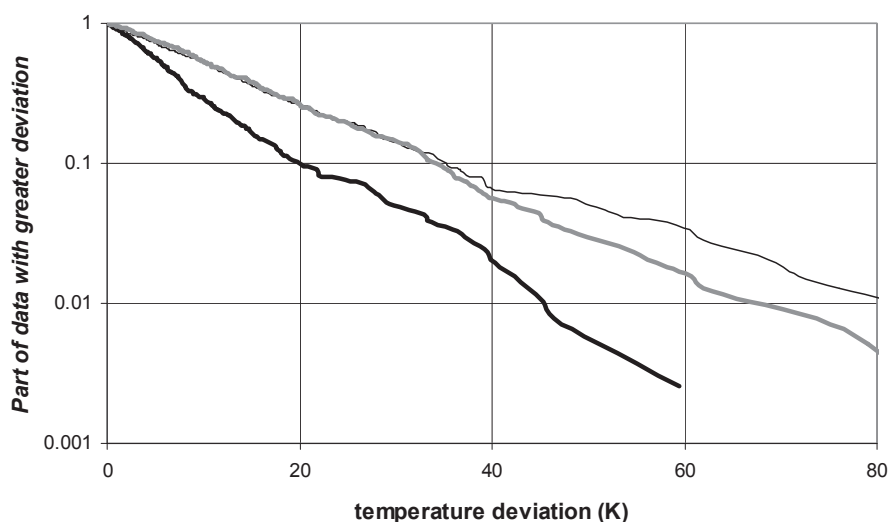


Figure 3.6.1. Fraction of the data with deviations larger than a given value for prediction of normal boiling point (NBP) of 386 compounds taken from Poling [83]; ( — ) the Joback and Reid method, ( — ) NBP predictions based on eq. (3.6.2) – (3.6.3) where  $W$  is the identity matrix, ( — ) the Joback-Reid distance weighting method JR-DW ( $W$  is from eq. (3.6.4) and (3.6.1)).

As can be seen, the DW method reduces the fraction of the database with deviations greater than a given value in comparison with the Joback and Reid method. In other words, the DW method increases the accuracy of NBP prediction. The improvement in NBP prediction is especially noticeable for small and large molecules ( $C_1$ - $C_3$ ,  $C_{21}$ - $C_{24}$ ).

## 4 Conclusions

The aim of this thesis was to investigate a set of binary systems to provide necessary thermodynamic data for the oil and biofuel industries. Reliable experimental and predicted thermodynamic data are the best foundation for the development and optimization of industrial processes. In natural product processing (as in the oil or forest industries), the number of process compounds is very large. There are still gaps in the available experimental thermodynamic data for systems consisting of process compounds. The thermodynamic data become even more important for processes related to the introduction of new gasoline additives or biofuels. Stricter control of gasoline impurities such as sulfur compounds also requires reliable thermodynamic data.

40 binary systems were investigated within this thesis. Several groups of the compounds investigated can be distinguished: alcohols, ketones, sulfur-containing compounds, and furfural. A number of measurement techniques (static total pressure apparatus, recirculation still, headspace gas chromatography) were successfully adapted for experiments with the investigated systems at wide ranges of pressures and temperatures. All the systems showed a positive deviation from Raoult's Law and in several binary systems, azeotropic behavior was observed.

Part of the work was related to measuring the phase behavior of furfural-containing binary systems. This aromatic aldehyde compound can be obtained in large amounts by the chemical processing of different wood and grass species and has been considered as the precursor of biofuel components. Four different types of apparatus were used for the measurement of thermodynamic properties. Because furfural reacts with atmospheric oxygen, the measurement procedures were modified to avoid furfural reactions. The techniques were also compared for their applicability for the measurement of reactive furfural. The VLE measurement of such systems with the different techniques not only provided important experimental data, but also enabled the development of thermodynamic models valid for the wide range of temperatures and pressures of the systems.

A substantial part of the work was dedicated to the validation of two predictive models with respect to the obtained experimental data. Two popular predictive models - UNIFAC (Dortmund) and COSMO-RS (COSMOlogic) - were compared based on their ability to predict the phase equilibria and excess enthalpy of the data obtained in the experimental work for this thesis. No significant difference was observed between the performances of the two models for the prediction of VLE behavior. UNIFAC (Dortmund) estimated the excess enthalpy slightly better than COSMO-RS. However, the description of the same property with empirical models (such as NRTL or

UNIQUAC) was usually considerably more accurate. This confirms the importance of experimental measurements and encourages the development of more accurate predictive methods.

A novel computational technique for the group contribution methods (GCMs) was suggested for improving the prediction of pure compound properties. Distance weighting is used in the novel method for optimizing group contribution parameters in accordance with the similarity between the estimated compound and the database compound. Test calculations based on the Joback – Reid and Marrero – Gani GCMs showed that the new technique improves the prediction of the test property (normal boiling point).



## References

- [1] Sandler SI. Chemical, biochemical, and engineering thermodynamics. 4th ed. ed. Hoboken, N.J: John Wiley; 2006.
- [2] Michelsen ML. A method for incorporating excess Gibbs energy models in equations of state. *Fluid Phase Equilib.* 1990;60(1-2):47-58.
- [3] Soave GS. Universal method for equations of state (UNIFEST): An application of UNIFAC to predict the parameters of cubic equations of state. *Fluid Phase Equilib.* 2002;193(1-2):75-86.
- [4] Jaubert J-, Mutelet F. VLE predictions with the Peng-Robinson equation of state and temperature dependent kij calculated through a group contribution method. *Fluid Phase Equilib.* 2004;224(2):285-304.
- [5] Soave G. Equilibrium constants from a modified Redlich-Kwong equation of state. *Chemical Engineering Science* 1972;27(6):1197-203.
- [6] Rackett HG. Equation of state for saturated liquids. *J.Chem.Eng.Data* 1970;15(4):514-7.
- [7] Kojima K, Man Moon H, Ochi K. Thermodynamic consistency test of vapor-liquid equilibrium data. - Methanol water, benzene ~ cyclohexane and ethyl methyl ketone ~ water -. *Fluid Phase Equilib.* 1990;56(C):269-84.
- [8] Kang JW, Diky V, Chirico RD, Magee JW, Muzny CD, Abdulagatov I, et al. Quality assessment algorithm for vapor-liquid equilibrium data. *J.Chem.Eng.Data* 2010;55(9):3631-40.
- [9] Behrens D, Gmehling J, Onken U. Chemistry data series. 1/1, Vapor-liquid equilibrium data collection. Aqueous-organic systems. Frankfurt/Main: DECHEMA; 1977.
- [10] Fredenslund A, Jones RL, Prausnitz JM. Group-contribution estimation of activity coefficients in nonideal liquid mixtures. *AIChE J.* 1975;21(6):1086-99.
- [11] Fredenslund A, Gmehling J, Michelsen ML, Rasmussen P, Prausnitz JM. Computerized design of multicomponent distillation columns using the UNIFAC group contribution method for calculation of activity coefficients. *Industrial and Engineering Chemistry Process Design and Development* 1977;16(4):450-62.
- [12] Skjold-Jørgensen S, Kolbe B, Gmehling J, Rasmussen P. Vapor-liquid equilibria by UNIFAC group contribution. Revision and extension. *Industrial and Engineering Chemistry Process Design and Development* 1979;18(4):714-22.
- [13] Gmehling J, Rasmussen P, Fredenslund A. Vapor-liquid equilibria by UNIFAC group contribution. Revision and extension. 2. *Industrial and Engineering Chemistry Process Design and Development* 1982;21(1):118-27.
- [14] Tiegs D, Gmehling J, Rasmussen P, Fredenslund A. Vapor-liquid equilibria by UNIFAC group contribution. 4. Revision and extension. *Industrial and Engineering Chemistry Research* 1987;26(1):159-61.
- [15] Hansen HK, Rasmussen P, Fredenslund A, Schiller M, Gmehling J. Vapor-liquid equilibria by UNIFAC group contribution. 5. Revision and extension. *Ind Eng Chem Res* 1991;30(10):2352-5.
- [16] Weidlich U, Gmehling J. Modified UNIFAC model. 1. prediction of VLE,  $H^E$ , and gamma infinity . *Ind Eng Chem Res* 1987;26(7):1372-81.
- [17] Gmehling J, Li J, Schiller M. Modified UNIFAC model. 2. Present parameter matrix and results for different thermodynamic properties. *Ind Eng Chem Res* 1993;32:178-93.

- [18] Gmehling J, Lohmann J, Jakob A, Li J, Joh R. A modified UNIFAC (Dortmund) model. 3. Revision and extension. *Ind. Eng. Chem. Res.* 1998;37:4876-82.
- [19] Wittig R, Lohmann J, Joh R, Horstmann S, Gmehling J. Vapor-liquid equilibria and enthalpies of mixing in a temperature range from 298.15 to 413.15 K for the further development of Modified UNIFAC (Dortmund). *Ind Eng Chem Res* 2001;40(24):5831-8.
- [20] Gmehling J, Wittig R, Lohmann J, Joh R. A modified UNIFAC (Dortmund) model. 4. Revision and extension. *Ind Eng Chem Res* 2002;41(6):1678-88.
- [21] Wittig R, Lohmann J, Gmehling J. Prediction of phase equilibria and excess properties for systems with sulfones. *AIChE J.* 2003;49(2):530-7.
- [22] Jakob A, Grensemann H, Lohmann J, Gmehling J. Further development of modified UNIFAC (Dortmund): Revision and extension 5. *Ind. Eng. Chem. Res.* 2006;45:7924-33.
- [23] Klamt A. Conductor-like Screening Model for Real Solvents: A New Approach to the Quantitative Calculation of Solvation Phenomena. *J. Phys. Chem.* 1995;99(7):2224-35.
- [24] Lucas K editor. *Molecular Models for Fluids.* : Cambridge University Press; 2007.
- [25] Klamt A, Krooshof GJP, Taylor R. COSMOSPACE: alternative to conventional activity-coefficient models. *AIChE J.* 2002;48(10):2332-49.
- [26] Klamt A. COSMO-RS: From Quantum Chemistry to Fluid Phase Thermodynamics and Drug Design. ; 2005.
- [27] Klamt A. *Cosmo-rs: From Quantum Chemistry to Fluid Phase Thermodynamics And Drug Design.* : Elsevier Science & Technology Books; 2005.
- [28] Klamt A, Jonas V, Buerger T, Lohrenz JCW. Refinement and Parametrization of COSMO-RS. *J. Phys. Chem. A* 1998;102(26):5074-85.
- [29] Eckert F, Klamt A. Fast solvent screening via quantum chemistry: COSMO-RS approach. *AIChE J.* 2002;48(2):369-85.
- [30] COSMOlogic GmbH & Co. COSMOtherm Version C2.1 Release notes (November 2009). Available at: <http://www.cosmologic.de/data/engineering/Release-Notes-COSMOtherm-C21-0110.pdf>, 2014.
- [31] "COSMOlogic GmbH & Co". COSMOtherm, Version C3.0, Release 12.01. 2012;
- [32] Jork C, Kristen C, Pieraccini D, Stark A, Chiappe C, Beste Y A, Arlt W. Tailor-made ionic liquids. *Journal of Chemical Thermodynamics.* 2005; 37(6): 537–558.
- [33] Buggert M, Cadena C, Mokrushina L, Smirnova I, Maginn EJ, Arlt W. COSMO-RS calculations of partition coefficients: Different tools for conformational search. *Chem.Eng.Technol.* 2009;32(6):977-86.
- [34] Spuhl O, Arlt W. COSMO-RS Predictions in Chemical Engineering-A Study of the Applicability to Binary VLE. *Ind. Eng. Chem. Res.* 2004;43(4):852-61.
- [35] Renon H, Prausnitz JM. Local compositions in thermodynamic excess functions for liquid mixtures. *AIChE J.* 1968;14:135-44.
- [36] Abrams DS, Prausnitz JM. Statistical thermodynamics of liquid mixtures: a new expression for the excess gibbs energy of partly or completely miscible systems. *AIChE J.* 1975;21(1):116-28.
- [37] Wilson GM. Vapor-liquid equilibrium. XI. A new expression for the excess free energy of mixing. *J.Am.Chem.Soc.* 1964;86(2):127-30.

- [38] Gmehling J, Li J, Schiller M. A modified UNIFAC model. 2. Present parameter matrix and results for different thermodynamic properties. *Ind. Eng. Chem. Res.* 1993;32(1):178-93.
- [39] Kolb B, Ettre LS. *Static headspace-gas chromatography : theory and practice*. New York : Wiley-VCH; 1997.
- [40] Uusi-Kyyny P, Pokki J-P, Laakkonen M, Aittamaa J, Liukkonen S. Vapor liquid equilibrium for the binary systems 2-methylpentane + 2-butanol at 329.2 K and n-hexane + 2-butanol at 329.2 and 363.2 K with a static apparatus. *Fluid Phase Equilib.* 2002;201(2):343-58.
- [41] Barker JA. Determination of activity coefficients from total pressure measurements. *Aust.J.Chem.* 1953;6:207-10.
- [42] Perry RH, Green DW. *Perry's Chemical Engineers' Handbook (7th Edition)*. 1997;.
- [43] Design institute for physical property data/AIChE. DIPPR Project 801. 2005/2008/2009;.
- [44] Thomson GH, Brobst KR, Hankinson RW. Improved correlation for densities of compressed liquids and liquid mixtures. *AIChE J.* 1982;28(4):671-6.
- [45] Reid RC, Prausnitz JM, Poling BE. *The properties of gases and liquids*. 4. ed. ed. New York: McGraw-Hill; 1987.
- [46] Taylor JR. *An introduction to error analysis : the study of uncertainties in physical measurements*. 2nd ed. ed. Sausalito (CA): University Science Books; 1997.
- [47] Laakkonen M, Pokki J-P, Uusi-Kyyny P, Aittamaa J. Vapour-liquid equilibrium for the 1-butene + methanol, + ethanol, + 2-propanol, + 2-butanol and + 2-methyl-2-propanol systems at 326 K. *Fluid Phase Equilib.* 2003;206(1-2):237-52.
- [48] Hynynen K, Uusi-Kyyny P, Pokki J-P, Pakkanen M, Aittamaa J. Isothermal vapor liquid equilibrium for 2-methylpropene + methanol, + 1-propanol, + 2-propanol, + 2-butanol, and + 2-methyl-2-propanol binary systems at 364.5 K. *J Chem Eng Data* 2006;51:562-8.
- [49] Yerazunis S, Plowright JD, Smola FM. Vapor-liquid equilibrium determination by a new apparatus. *AIChE J.* 1964;10(5):660-5.
- [50] Uusi-Kyyny P, Pokki J-P, Aittamaa J, Liukkonen S. Vapor - Liquid Equilibrium for the Binary Systems of Methanol + 2,4,4-Trimethyl-1-pentene at 331 K and 101 kPa and Methanol + 2-Methoxy-2,4,4-trimethylpentane at 333 K. *J.Chem.Eng.Data* 2001 09/01; 2013/10;46(5):1244-8.
- [51] Agilent Technologies Inc. *Documentation for Agilent Technologies 7697A Headspace Sampler, Advanced Operation*. Wilmington, USA: Agilent Technologies Inc.; 2011.
- [52] Westerholt A, Liebert V, Gmehling J. Influence of ionic liquids on the separation factor of three standard separation problems. *Fluid Phase Equilib.* 2009 6/25;280(1-2):56-60.
- [53] Luis P, Wouters C, Sweygens N, Creemers C, Van der Bruggen B. The potential of headspace gas chromatography for VLE measurements. *The Journal of Chemical Thermodynamics* 2012 6;49(0):128-36.
- [54] Wadsö I, Goldberg RN. Standards in isothermal microcalorimetry: (IUPAC Technical Report). *Pure Appl.Chem.* 2001;73(10):1625-39.
- [55] Aittamaa J, Pokki J-P, User Manual of Program VLEFIT. 2003; Technical University of Helsinki  
Espoo.  
[http://chemtech.aalto.fi/en/research/groups/chemical\\_engineering/software/vlefit/](http://chemtech.aalto.fi/en/research/groups/chemical_engineering/software/vlefit/)
- [56] Fredenslund A, Gmehling J, Rasmussen P. *Vapor-Liquid Equilibria Using UNIFAC, a Group-Contribution Method*. 1977; Elsevier, Amsterdam.

- [57] Davidon WC, Optimally conditioned optimization algorithms without line searches. *Math. Program.* 1975; 9: 1–30.
- [58] COSMOlogic GmbH & Co. COSMOtherm Version C2.1 Release Notes (November 2008). Available at: <http://www.cosmologic.de/data/engineering/Release-Notes-C21-0108.pdf>, 2014.
- [59] Hypercube I. Molecular Modeling System, Hyperchem. Hyperchem 2002;7.52 for Windows.
- [60] Stewart JJP. Optimization of parameters for semiempirical methods I. *Method. Journal of Computational Chemistry* 1989;10(2):209-20.
- [61] Mu T, Rarey J, Gmehling J. Performance of COSMO-RS with sigma profiles from different model chemistries. *Ind. Eng. Chem. Res.* 2007;46:6612-29.
- [62] Xue Z, Mu T, Gmehling J. Comparison of the a Priori COSMO-RS models and group contribution methods: Original UNIFAC, modified UNIFAC(Do), and modified UNIFAC(Do) consortium. *Ind Eng Chem Res* 2012;51(36):11809-17.
- [63] Grensemann H, Gmehling J. Performance of a conductor-like screening model for real solvents model in comparison to classical group contribution methods. *Ind. Eng. Chem. Res.* 2005;44:1610-24.
- [64] Constantinescu D, Rarey J, Gmehling J. Application of COSMO-RS Type Models to the Prediction of Excess Enthalpies. *Ind. Eng. Chem. Res.* 2009;48(18):8710-25.
- [65] McFall TA, Post ME, Collins SG, Christensen JJ, Izatt RM. The excess enthalpies of 10 (n-butane + alcohol) mixtures at 298.15 K. *J Chem Thermodyn* 1981;13(1):41-6.
- [66] Sipowska JT, Ott JB, Woolley AT, Izatt RM. Excess enthalpies for (butane + methanol) at the temperatures (298.15, 323.15, and 348.15) K and the pressures (5 and 15) MPa. *J Chem Thermodyn* 1992;24(10):1087-93.
- [67] Sipowska JT, Lemon LR, Ott JB, Brown PR, Marchant BG. Excess enthalpies and excess volumes for (butane + butan-1-ol) at the temperatures (298.15, 323.15, and 348.15) K and pressures (5, 10, and 15) MPa. *The Journal of Chemical Thermodynamics* 1994 12;26(12):1275-86.
- [68] Moore JD, Brown PR, Ott JB. Excess molar enthalpies and excess molar volumes for the binary mixtures of 2-methylpropane, 2-methylpropene, and propan-2-ol at the temperatures (298.15 and 323.15) K and the pressures (5,10, and 15) MPa. *J Chem Thermodyn* 1997;29(2):179-95.
- [69] Schafer K, Rohr FJ. Thermal investigations of mixtures of acetone with normal hydrocarbons. *Z.Phys.Chem.(Muenchen, Ger.)* 1960;24:130-51.
- [70] Chao JP, Dai M. Studies of thermodynamic properties of binary mixtures containing an alcohol XVI. excess molar enthalpies of each of (one of the four butanols + methyl ethyl ketone or methyl isobutyl ketone) at the temperature 298.15 K. *J Chem Thermodyn* 1991;23(2):117-21.
- [71] Solimo H, Riggio R, Martinez H. Excess thermodynamic properties for methyl isobutyl ketone + tert-amyl alcohol system at 25 Å°C. *Journal of Solution Chemistry* 1986 03/01;15(3):283-9.
- [72] Naorem H, Suri SK. Excess molar enthalpies for binary liquid mixtures of furfural with some aliphatic alcohols. *J.Chem.Eng.Data* 1989 10/01; 2012/10;34(4):395-7.
- [73] Behrens D, Christensen C. Chemistry data series. 3/1, Heats of mixing data collection. Binary systems. Frankfurt/Main: DECHEMA; 1984.

- [74] Ferhat-Hamida Z, Philippe R, Merlin JC, Kehiaian HV. Thermodynamic properties of binary mixtures containing thiaalkanes. I. Excess enthalpies of n-thiaalkane + n-alkane mixtures. *J.Chim.Phys.Phys.-Chim.Biol.* 1979;76(2):130-6.
- [75] Didaoui-Nemouchi S, Ait Kaci A. Molar excess enthalpies of thiophene and diethyl sulfide binary mixtures with n-alkanes. *J Therm Anal Calor* 2002;69(2):669-80.
- [76] Marongiu B, Marras G, Pittau B, Porcedda S. Thermodynamics of binary mixtures containing thiaalkanes. Excess enthalpies of thiaalkanes and polythiaalkanes + n-alkanes or cyclohexane. *Fluid Phase Equilib.* 1994;97:127-46.
- [77] Moore JD, Brown PR, Ott JB. Excess molar enthalpies and excess molar volumes for the binary mixtures of 2-methylpropane, 2-methylpropene, and propan-2-ol at the temperatures (298.15 and 323.15) K and the pressures (5, 10, and 15) MPa. *J Chem Thermodyn* 1997;29(2):179-95.
- [78] Ferhat-Hamida Z, Philippe R, Merlin JC, Kehiaian HV. Thermodynamic properties of binary mixtures containing thiaalkanes. I. Excess enthalpies of n-thiaalkane + n-alkane mixtures. *J.Chim.Phys.Phys.-Chim.Biol.* 1979;76(2):130-6.
- [79] DDBST GmbH. Online Dortmund Data Bank Search. 2013;.
- [80] The National Institute of Standards and Technology. Thermolite, NIST Literature Report Builder. 2013;.
- [81] Joback KG, Reid RC. Estimation of pure-component properties from group contributions. *Chem. Eng. Commun.* 1987;57(1-6):233-43.
- [82] Marrero J, Gani R. Group-contribution based estimation of pure component properties. *Fluid Phase Equilib.* 2001 7/1;183-184:183-208.
- [83] Poling BE, Prausnitz JM, O'Connell JP. *Properties of Gases and Liquids (5th Edition)*. : McGraw-Hill; 2001.



ISBN 978-952-60-5750-7  
ISBN 978-952-60-5751-4 (pdf)  
ISSN-L 1799-4934  
ISSN 1799-4934  
ISSN 1799-4942 (pdf)

**Aalto University**

**Department of Biotechnology and Chemical Technology**  
[www.aalto.fi](http://www.aalto.fi)

**BUSINESS +  
ECONOMY**

**ART +  
DESIGN +  
ARCHITECTURE**

**SCIENCE +  
TECHNOLOGY**

**CROSSOVER**

**DOCTORAL  
DISSERTATIONS**